

### **Highlights**

1. The mean soil organic carbon (SOC) is lower in the Sundarbans than most mangroves.
2. Both salinity zone and forest type had a significant effect on SOC.
3. Irrespective of salinity zonation, the top 10 cm contained the highest SOC density.
4. Salinity, C: N and tree diameter were the best predictors of SOC variability.

1           **Is soil organic carbon underestimated in the largest mangrove forest**  
2                           **ecosystems? Evidence from the Bangladesh Sundarbans**

3  
4   Md. Saidur Rahman<sup>a, b, \*</sup>, Daniel N.M. Donoghue<sup>a</sup>, Louise J. Bracken<sup>a</sup>

5  
6   <sup>a</sup>Department of Geography, Durham University, South Road, Durham DH1 3LE, United Kingdom.

7  
8   <sup>b</sup>Forestry and Wood Technology Discipline, Khulna University, Khulna-9208, Bangladesh

9

10

11

12   Corresponding author \*: msrahman@fwt.ku.ac.bd

13

## Abstract

14 Globally, mangroves sequester a large amount of carbon into the sediments, although spatial  
15 heterogeneity exists owing to a wide variety of local, regional, and global controls. Rapid environmental  
16 and climate change, including increasing sea-level rise, global warming, reduced upstream discharge  
17 and anthropogenic activities, are predicted to increase salinity in the mangroves, especially in the  
18 Bangladesh Sundarbans, thereby disrupting this blue carbon reservoir. Nevertheless, it remains unclear  
19 how salinity affects the belowground soil carbon despite the recognised effect on above ground  
20 productivity. To address this gap, research was undertaken in the Bangladesh Sundarbans to compare  
21 total soil organic carbon (SOC) across three salinity zones and to explore any potential predictive  
22 relationships with other physical, chemical properties and vegetation characteristics. Total SOC was  
23 significantly higher in the oligohaline zone ( $74.8 \pm 14.9 \text{ Mg ha}^{-1}$ ), followed by the mesohaline ( $59.3 \pm$   
24  $15.8 \text{ Mg ha}^{-1}$ ), and polyhaline zone ( $48.3 \pm 10.3 \text{ Mg ha}^{-1}$ ) (ANOVA,  $F_{2, 500} = 118.9$ ,  $p < 0.001$ ). At all  
25 sites, the topmost 10 cm of soil contained higher SOC density than the bottom depths (ANOVA,  $F_{3, 500}$   
26  $= 30.1$ ,  $p < 0.001$ ). On average, *Bruguiera sp.* stand holds the maximum SOC measured, followed by  
27 two pioneer species *Sonneratia apetala* and *Avicennia sp.* Multiple regression results indicated that soil  
28 salinity, organic C: N and tree diameter were the best predictor for the variability of the SOC in the  
29 Sundarbans ( $R^2 = 0.62$ ). Despite lower carbon in the soil, the study highlights that the conservation  
30 priorities and low deforestation have led to less CO<sub>2</sub> emissions than most sediment carbon-rich  
31 mangroves in the world. The study also emphasised the importance of spatial conservation planning to  
32 safeguard the soil carbon-rich zones in the Bangladesh Sundarbans from anthropogenic tourism and  
33 development activities to support climate change adaptation and mitigation strategies.

34 **Keywords:** Soil organic carbon; salinity zones; soil depth; mangrove forest; the Sundarbans.

## 1. Introduction

35 Mangroves are recognised as one of the most carbon-dense forest types in the world due to their efficient  
36 carbon sequestration capacity into both above and below ground carbon pools (Donato et al., 2011;  
37 Alongi, 2012; Sanderman et al., 2018). Recent assessments of soil carbon suggest that mangrove  
38 ecosystems contain, on an average, between 856 and 1,023 Mg of carbon per hectare, with the majority  
39 (~85%) of this carbon stored in the soil (Donato et al., 2011; Pendleton et al., 2012; Sanderman et al.,  
40 2018; Kauffman et al., 2020). This large amount of soil carbon is of global importance due to its  
41 potential to store sequestered CO<sub>2</sub> emissions for the long term and help mitigate adverse effects of  
42 climate change (McLeod et al., 2011; Duarte et al., 2013; Abdullah et al., 2016). To recognise the  
43 importance of mangrove forests for carbon sequestration, United Nations Environmental Programme  
44 (UNEP) designated this ecosystem as “Blue Carbon” along with other coastal vegetated ecosystems  
45 such as seagrass meadows and saltmarshes (Nellemann et al., 2009; Lovelock and Duarte, 2019;  
46 Macreadie et al., 2019). This growing worldwide importance of mangroves has led to a substantial  
47 reduction of mangrove loss leading to reductions in CO<sub>2</sub> emissions in the last three decades (Friess et  
48 al., 2019). At the same time, mangroves have gained substantial traction in being managed, protected  
49 and restored as part of national and global climate change mitigation policies and actions including  
50 Nationally Determined Contributions (NDC) towards the Paris Agreement and climate action goal (goal  
51 13) under United Nations Sustainable Development Goals (SDG) (Taillardat et al., 2018; Friess et al.,  
52 2020). However, variability and uncertainty in SOC estimation is a key barrier to the inclusion of  
53 mangroves (and other blue carbon) in national and international policy tools and frameworks.

54 Despite covering only 0.1% of the world’s total landmass, mangroves sequester more carbon per unit  
55 area than any other natural ecosystems (Atwood et al., 2017; Lovelock and Duarte, 2019). With  
56 autochthonous inputs from the productive above-ground, mangrove soils store large quantities of carbon  
57 as a result of the low decomposition rate resulting from anoxic conditions (Donato et al., 2011; Alongi,  
58 2012). Mangroves are also highly efficient traps for allochthonous inputs through their dense network  
59 of above ground roots. The rising elevation of mangroves in response to sea-level rise allows large  
60 accommodation spaces to sequester more carbon in the soil, which barely reaches saturation (Krauss et

61 al., 2014; Rogers et al., 2019). Therefore, mangroves act as an efficient carbon store despite continuous  
62 threats from deforestation, land-use change, sea-level rise, and climate change.

63 Blue carbon research across the globe has highlighted considerable spatial heterogeneity in soil organic  
64 carbon (SOC) at multiple scales (Atwood et al., 2017; Sanderman et al., 2018). At a regional and global  
65 scale, SOC variability has been linked to net primary productivity (Alongi, 2012; Twilley et al., 2017),  
66 latitude/climate (Rovai et al., 2018; Twilley et al., 2018; Kauffman et al., 2020), coastal geomorphology  
67 (Rovai et al., 2018; Twilley et al., 2018) and Holocene sea-level trends (Rogers et al., 2019). These  
68 physical and biological factors and geomorphic evolutionary processes promote and develop unique  
69 coastal environmental settings, which ultimately drive macroscale variation in SOC (Rovai et al., 2018).  
70 The site-specific variability in SOC is largely attributed to differences in species composition (Ren et  
71 al., 2008), stand age (Lovelock et al., 2010; Donato et al., 2011), sources of allochthonous particles  
72 (Bouillon and Boschker, 2006; Yang et al., 2014), soil physical and chemical properties (Freeman et  
73 al., 2004; Kristensen et al., 2008; Banerjee et al., 2018), elevation and tidal regimes (Liu and Lee, 2006;  
74 Spivak et al., 2019), plant-litter biochemistry (Kristensen et al., 2008; Brodersen et al., 2019) and plant-  
75 microbe interactions (Fontaine et al., 2007; Alongi, 2014). Several soils and environmental  
76 characteristics such as pH, salinity, organic matter, precipitation and tidal inundation influence the  
77 mangrove productivity and can also directly or indirectly influence SOC (Yando et al., 2016).  
78 Therefore, careful consideration of relevant factors is vital for reliable estimation of SOC at a particular  
79 spatial scale.

80 The Sundarbans is the largest contiguous mangrove forest in the world and is situated in the lower delta  
81 plain of the Ganges-Brahmaputra-Meghna (GBM) delta, and stretches across political boundaries  
82 between Bangladesh and India (Giri et al., 2011; Sarker et al., 2016). It is either mostly excluded from  
83 the global estimates of mangrove SOC (Table 1), or is underrepresented due to a limited number of  
84 samples or perceived poor data quality (Donato et al., 2011; Jardine and Siikamäki, 2014; Atwood et  
85 al., 2017; Sanderman et al., 2018; Twilley et al., 2018; Kauffman et al., 2020). A range of studies into  
86 SOC content in mangrove soils of the Sundarbans have been carried out (Table 1), but these all have  
87 limitations. The first comprehensive carbon inventory throughout the Sundarbans was completed by the

88 Bangladesh Forest Department (BFD) in 2009-10; however, the wider vertical sample depth might have  
89 an effect on the SOC estimation within the top meter (Rahman et al., 2015). Allison et al. (2003) and  
90 Donato et al. (2011) investigated soil organic carbon at greater depth (>1 m) in the Bangladesh  
91 Sundarbans, however, the number of samples (2 and 6 respectively) was not sufficient to address the  
92 variability inside the forests. Studies by Khan and Amin (2019) and Hossain and Bhuiyan (2016)  
93 measured SOC from different parts of the Sundarbans, however, the sampling was only performed  
94 within the top 15 cm. These all the previous studies of SOC in the Sundarbans have limitations resulting  
95 from low spatial sampling intensity and limited analysis of soil depth range. Moreover, some global  
96 studies like Rovai et al. (2018) argued that past climate-based estimation overestimated SOC by up to  
97 86% for deltaic settings like the Sundarbans. Therefore, accurate investigation on the spatial variation  
98 of soil organic carbon and the identification of major controls for such variation in the Bangladesh  
99 Sundarbans is urgently needed.

100 Increasing salinity in the inundated mangroves stimulate a wide range of biogeochemical reactions-  
101 including enhancing sulphate concentrations, cation exchange, ionic and osmotic stress, acidity, and  
102 turbidity and at the same time reducing soil redox potential and oxygen levels (Setia et al., 2013; Luo  
103 et al., 2019). These soil biogeochemical changes in turn alter sediment characteristics and modify plant  
104 and microbe communities, which ultimately affect both the soil organic carbon pool and quality.  
105 Increased soil salinity affects organic matter solubility by altering flocculation of different soil particles  
106 (Wong et al., 2009; Wong et al., 2010; Rath and Rousk, 2015). The Investigations of tidal wetlands  
107 across the world reveals a significant negative relationship between the soil organic carbon pool with  
108 salinity (Nyman et al., 1990; Craft, 2007; Więski et al., 2010; Morrissey et al., 2014; Hu et al., 2016).  
109 High soil salinity decreases decomposition rates by lowering microbial activities in the soil and lowers  
110 autochthonous carbon input by reducing plant productivity leading to lower organic carbon in the soil  
111 (Baldwin et al., 2006; Marton et al., 2012; Setia et al., 2013; Liu et al., 2017; Zhao et al., 2017). High  
112 salinity in general acts as an inhibitor of carbon mineralisation, however the opposite is also evident in  
113 some studies suggesting that a small increase in salinity promotes mineralisation process in the  
114 oligohaline zone, while in the mesohaline and polyhaline zones, elevated salinity reduces the

115 mineralisation rate (Luo et al., 2019). Therefore, the impact of salinity on the soil organic carbon pool  
116 and quality is not uniform in all wetland settings in the world, rather it depends on the local  
117 geomorphology and hydrological characteristics.

118 The aim of the present study is to estimate soil organic carbon (SOC) in the Bangladesh part of the  
119 Sundarbans mangrove forest and to better understand the relationship of SOC with three salinity zones  
120 (oligohaline, mesohaline and polyhaline) and major forest types. The study hypothesises that higher  
121 salinity zones (polyhaline) would yield a lower organic soil carbon stock as a reflection of lower  
122 productive vegetation and altered soil physical and biological processes compared with the lower  
123 salinity zone (oligohaline). The relationships between physical, chemical properties and vegetation  
124 characteristics with SOC are also investigated to develop dependable predictive models for this forest.  
125 The novelty of this study lies in the extensive stratified random sampling from all over Bangladesh  
126 Sundarbans combined with vertical investigation of soil depth up to 1m.

## 2. Material and methods

### 127 2.1. Study area

128 The Sundarbans is the largest single block of mangrove forest in the world and a Ramsar and UNESCO  
129 World Heritage site (Fig. 1) (Giri et al., 2011; Sarker et al., 2016). The Bangladesh Sundarbans is  
130 situated between 21°30' N and 22°30' N and 89°00' E and 89°55' E. The climate of the Sundarbans is  
131 warm, humid, and tropical, where annual precipitation varies from 1474 to 2265 mm and mean annual  
132 minimum and maximum temperature is between 29 °C to 31 °C (Chowdhury et al., 2016; Sarker et al.,  
133 2016). Based on the salinity variation, the Sundarbans naturally divides into three distinct zones based  
134 on the soil salinity; i) Oligohaline (LSZ) (<2 dS/m, ii) Mesohaline (2-4 dS/m) and iii) Polyhaline (>4  
135 dS/m) (Siddiqi, 2001; Chanda et al., 2016b). Several studies have identified a relationship between tree  
136 species abundance along the east-west salinity gradient (Iftekhar and Saenger, 2008; Aziz and Paul,  
137 2015; Sarker et al., 2016; Sarker et al., 2019a). Although *Excoecaria agallocha* is abundant in all three  
138 salinity zones, *Heritiera fomes* (characteristic species in Bangladesh Sundarbans) is dominant in both  
139 the oligohaline and mesohaline zones, whereas *Ceriops decandra* is abundant in the polyhaline zone

140 (Sarker et al., 2019a). Some pioneer species, such as *Avicenna* spp. and *Sonneratia apetala* are also  
141 present in the mudflats all over the Sundarbans. A short description of all 23 tree species from 10  
142 families found in this study is presented in Table A.1.

## 143 **2.2. Geology and soils of the Sundarbans**

144 The Sundarbans mangrove forest lies in the south-western part of the Bengal Basin, one of the most  
145 extensive sediment reservoirs in the world composed of unconsolidated Quaternary deposits (Rudra,  
146 2014). The rapid sedimentation followed by the tectonic collision of the Indian plate with the Tibetan  
147 plate and the Burmese plate in the Miocene triggered the formation of the Bengal Basin (Alam, 1989).  
148 Since the Holocene, the dynamic Ganges-Brahmaputra river system has been discharging sediments  
149 from the Sub-Himalaya and is still delivering >1 Gt of sediment to the delta plain of India and  
150 Bangladesh (Islam et al., 1999; Syvitski and Milliman, 2007). The Sundarbans is of relatively recent  
151 origin (3,000-year B.P.) and this mangrove has developed as a result of both fluvial and tidal forces  
152 depositing sediments to the GBM river mouth (Goodbred and Kuehl, 2000; Allison and Kepple, 2001;  
153 Rogers et al., 2013). Previously, the Ganges was the main source of sediments in the Sundarbans,  
154 however, recent changes have resulted from the merging of the Ganges and Brahmaputra which have  
155 now migrated to the eastward, far away from the Sundarbans (Rudra, 2014; Islam, 2016). Together with  
156 the eastward migration of the primary GBM delta, the construction of the Farakka barrage in the main  
157 Ganges River and earthen embankments surrounding the Sundarbans have reduced freshwater flow,  
158 resulting in reduced fluvial sedimentation in the Bangladesh Sundarbans. This geomorphological  
159 change, in turn, has led to increased remobilisation of sediments by tidal forces (Rogers et al., 2013;  
160 Hale et al., 2019; Bomer et al., 2020b). The changed pattern of freshwater flow has resulted in a salinity  
161 gradient increasing from the east to the west of the Sundarbans.

162 The soil is mainly fine-grained, grey coloured, slightly calcareous, and mostly composed of silts to  
163 clayey silts (Allison et al., 2003; Bomer et al., 2020a). The subsurface sediment extends up to 6 m in  
164 depth in the landward direction and up to 4 m in depth in the seaward direction (Allison et al., 2003).  
165 The median grain size ranges between 16-32  $\mu\text{m}$  reflecting the medium silt range. The average dry bulk  
166 density ( $0.81 \text{ g cm}^{-3}$ ) is higher in the Sundarbans in comparison to other mangroves in the world (Bomer

167 et al., 2020a). The soil physical and chemical properties are varied from the eastern to the western part  
168 of Bangladesh Sundarbans, the eastern part is softer, more fertile and receives more fresh sediments  
169 than the western part (Siddiqi, 2001). Soils are mostly neutral to alkaline (pH 6.5-8.0), whereas the  
170 polyhaline zone is more alkaline than the oligohaline zone. Soils of the western and southern polyhaline  
171 zone are comparatively richer in P, K, Na, Mg, Cl<sup>-</sup> and Fe, but lower in soil NH<sup>4+</sup> and Na than the eastern  
172 oligohaline zone (Siddiqi, 2001; Sarker et al., 2016). This pronounced differences in soil nutrients and  
173 salinity trigger the diversity of vegetation composition in different parts of the Sundarbans.

### 174 **2.3. Sediment and tree data collection**

175 In the Bangladesh Sundarbans, permanent sample plots (PSP) were established in 1986 by the ODA  
176 (Overseas Development Administration) for monitoring growth, regeneration, and long-term ecological  
177 changes (Chaffey et al., 1985). A total of 120 PSPs (20 m × 100 m) were established to assess growth  
178 rate, regeneration, stocking, and crop composition based on salinity, forest type and accessibility  
179 (Iftekhar and Saenger, 2008; Sarker et al., 2019b) (Fig. 1). In this study, sediment samples were  
180 collected from 55 plots, of which 50 plots are from PSPs selected at random, and the remaining five  
181 plots are from outside PSPs to represent areas outside PSP. Sampling was undertaken in two phases: In  
182 the first phase, three sediment cores of 50 cm depth were taken from 18 PSPs. After laboratory analysis  
183 of the samples from the first 18 PSPs, it was decided to extend the sediment sampling depth to 1 m and  
184 take two core samples from each plot because of little within-plot variation among the initial 54 core  
185 samples. In the second phase, an additional 37 PSPs were sampled with two cores sampled at each plot.  
186 Altogether, 126 sediment cores from 55 plots were sampled across the whole of the Bangladesh  
187 Sundarbans (Fig. 1).

188 The location of the cores within a PSP was decided by establishing a random circular plot with a radius  
189 of 11.3 m (an area of 400 m<sup>2</sup>). Within each plot, a small circular plot was laid with 5m radius and  
190 sediment cores were taken from east, west and south side (east and west for two cores) from the centre,  
191 which is perpendicular to each other. The cores were taken using an open-faced auger (6 cm diameter),  
192 which was further subdivided into four depths (0-10, 10-30, 30-50 and 50-100 cm), following the  
193 method of Kauffman and Donato (2012). Sediment sub-samples were taken from the middle of each

194 core section with fixed 2.5 cm length, sealed in plastic and subsequently placed in an icebox to reduce  
195 oxidation. The sub-samples were kept below 4 °C in zip-sealed plastic bags until laboratory processing.  
196 For vegetation data, the Diameter at Breast Height (DBH) and height were measured for all trees within  
197 the 11.3 m radius plot. DBH was measured at 1.3 m and height was measured with a Vertex-III  
198 hypsometer. For small trees with a DBH <14.5 cm, a smaller circular plot (radius 5m) was nested within  
199 the 11.3 m plot. The elevation of each plot was calculated by subtracting the mean tree height of the  
200 plot from the Digital Surface Model (DSM) taken from the TanDEM-X 90 m satellite data (Hawker et  
201 al., 2019). For major forest types, single-species dominance was determined when the relative  
202 composition is >75%, and the remaining forest types are termed as Mixed type.

## 203 **2.4. Laboratory analysis**

### 204 **2.4.1 Soil physical and chemical properties**

205 For each core sub-samples, samples were freeze-dried and re-weighted to determine the bulk density.  
206 Bulk density was calculated by dividing the dry mass of the soil by the volume of the soil. Soil pH and  
207 soil salinity (as soil conductivity) were measured from a portion of the homogenised dry soil for each  
208 core. Dried soils were diluted with distilled water (1:5 ratio), and subsequently, soil pH was measured  
209 using a Jenway 3510 Standard Digital pH Meter and soil salinity by a handheld Jenway 470  
210 Conductivity Meter (Hardie and Doyle, 2012).

### 211 **2.4.2 Total soil organic carbon (SOC)**

212 To determine the soil organic carbon (SOC) and nitrogen content of the soil, any large stones or twigs  
213 were removed from the sample and subsequently homogenised and ground with a ball mill. A few  
214 milligrams (~40 mg) of the sediment was then passed through an elemental analyser (Thermo  
215 Scientific Flash 2000-NC Soil Analyzer) to derive the total carbon and nitrogen as a percentage.  
216 Inorganic carbon content was deducted from the total carbon to get organic carbon percentage,  
217 according to Howard et al. (2014). The inorganic carbon content was measured from some random  
218 samples across all salinity zones using an Analytik Jena Multi EA (Elemental Analyser) 4000. Soil

219 organic carbon density ( $\text{gm cm}^{-3}$ ) for each sample and total organic carbon content ( $\text{Mg ha}^{-1}$ ) of each  
220 depth and core were measured according to Howard et al. (2014).

## 221 **2.5. Statistical Analysis**

222 All statistical analysis and graphics used R 3.6.1 for Windows (R Core Team, 2019). Total organic  
223 carbon ( $\text{Mg ha}^{-1}$ ), organic carbon density ( $\text{gm cm}^{-3}$ ) and bulk density ( $\text{gm cm}^{-3}$ ) among three salinity  
224 zones and four depths were compared with two-way analysis of variance (ANOVA) test using the ‘car’  
225 package (Fox and Weisberg, 2019). In order to compare soil organic carbon among vegetation types,  
226 total organic carbon ( $\text{Mg ha}^{-1}$ ) was compared with one-way analysis of variance (ANOVA). The results  
227 of ANOVA are summarized in Supplementary Information. To derive the relationship among organic  
228 carbon density ( $\text{g cm}^{-3}$ ), bulk density and total nitrogen content, data from all the core subsections ( $n =$   
229 512) were used. To examine the relationship among SOC and soil physical and chemical parameters  
230 (soil salinity, pH, bulk density, Total N, organic C: N, elevation, latitude and longitude) and vegetation  
231 characteristics (species richness, tree density, mean DBH and mean height), stepwise multiple linear  
232 regression analysis was undertaken. SOC was considered as the dependant variable, whereas all the  
233 selected parameters were independent variables. Correlation analysis and principal component analysis  
234 (PCA) were carried out to decrease the number of explanatory variables and to reduce collinearity in  
235 the regression model. All the variables were standardised before PCA according to Legendre and  
236 Legendre (2012). Eigenvalues greater than one were retained and variables with factor loadings  $>0.35$   
237 were treated as potential explanatory variables for the regression model (Jackson, 1993). In all cases,  
238 the data were logarithmic (natural) transformed (if needed) to meet the assumptions of normality and  
239 equal variances by using Shapiro Wilk and Levene’s tests, respectively and subsequently back-  
240 transformed to present graphically. The graphical output of the linear model was generated using the  
241 ‘ggplot2’ package (Wickham, 2016).

## **3. Results**

### 242 **3.1. Soil organic carbon, salinity zones and soil depth**

243 The average soil organic carbon (SOC) density significantly varied from 0.003 gm cm<sup>-3</sup> to 0.009 gm  
244 cm<sup>-3</sup> in different salinity zones and soil depths (two-way ANOVA for Ln (SOC density), salinity zones,  
245  $F_{2, 500} = 112.3, p < 0.001$  and soil depths,  $F_{3, 500} = 30.1, p < 0.001$ ) (Fig. 2, Table A.2). Both salinity zone  
246 and soil depth had a significant interaction effect on the variability of SOC density in the Sundarbans  
247 ( $F_{6, 500} = 3.5, p < 0.01$ ) (Table A.1). Significantly higher SOC density was found in the topmost depth  
248 followed by the subsequent three depths; however, SOC density in the intermediate depths (between  
249 10-30 cm and 30-50 cm) are not significantly different (Fig. 2b), which indicates the unequal variability  
250 of SOC with soil depth. The oligohaline zone comprises higher SOC density (gm cm<sup>-3</sup>) followed by  
251 mesohaline and polyhaline zone indicating higher soil organic carbon in the low salinity areas.

252 The bulk density (BD) of the soil revealed an opposite trend as significantly higher bulk density was  
253 observed in the higher salinity zones and in the 50-100 cm soil depth (two-way ANOVA for Ln (bulk  
254 density (gm cm<sup>-3</sup>)), salinity zones,  $F_{2, 500} = 22.2, p < 0.001$  and soil depth,  $F_{3, 500} = 46.2, p < 0.001$ ) (Fig.  
255 A.1, Table A.3). Likewise, SOC density, the soil organic carbon storage (SOC) for the different depths  
256 was significantly different among the three salinity zones and the four soil depths (two-way ANOVA  
257 for Ln (SOC), salinity zones,  $F_{2, 500} = 118.9, p < 0.001$  and soil depth,  $F_{3, 500} = 526.2, p < 0.001$ ) (Fig. 3 &  
258 Fig. 4, Table A.4). However, higher amounts of SOC were found in the 50-100 cm depth in comparison  
259 to the top three depths (Fig. 4). The top meter SOC ranges from 26.2 Mg ha<sup>-1</sup> to 107.9 Mg ha<sup>-1</sup> in the  
260 Sundarbans, where oligohaline zone comprises the highest SOC (74.8 Mg ha<sup>-1</sup>), followed by the  
261 mesohaline (59.3 Mg ha<sup>-1</sup>), and the polyhaline zone (48.3 Mg ha<sup>-1</sup>) (Table 2).

### 262 **3.2. Soil organic carbon and forest types**

263 One-way ANOVA revealed that SOC varied with major forest types in the Sundarbans ( $F_{7, 47} = 3.3, p$   
264  $< 0.01$ ) (Table A.5). As shown in Fig. 5, the average SOC content in the *Bruguiera* sp. stand was the  
265 highest, with an average of 105.3 Mg ha<sup>-1</sup>, followed by *Sonneratia* sp. and *Avicennia* sp., with an  
266 average of 68.7 Mg ha<sup>-1</sup> and 67.1 Mg ha<sup>-1</sup>, respectively. The Tukey HSD test showed that the other  
267 forest types had no significant effect on SOC content, which ranges from 50.2 Mg ha<sup>-1</sup> to 67.0 Mg ha<sup>-1</sup>  
268 for *Ceriops* and *Heritiera* forest types, respectively (Table A.6).

### 269 **3.3. Soil physical, chemical properties and vegetation characteristics**

270 The soil physical, chemical properties and vegetation characteristics vary considerably among the three  
271 salinity zones (Table 2). As expected, oligohaline zones had relatively low average soil bulk density,  
272 pH, and soil salinity, in comparison to higher salinity zones. Additionally, significantly higher SOC and  
273 lower total N contributes higher organic C: N in the oligohaline zone, although it is similar to the  
274 mesohaline zone ( $p < 0.05$ ). BD and SOC density showed a statistically significant negative relationship  
275 ( $r = -0.47, p < 0.001$ ) (Fig. 6A). However, the soil organic carbon (SOC) density and soil nitrogen density  
276 is significantly positively correlated with soil nitrogen density across the Sundarbans ( $r = 0.66, p$   
277  $< 0.001$ ) (Fig. 6B). Analysis from the satellite and tree height data reveals that the average elevation is  
278 higher in the polyhaline zone. The average DBH and height of the trees were statistically significantly  
279 higher in both the oligohaline and mesohaline zone, whereas the average stem density was higher in  
280 both the mesohaline and polyhaline zone ( $p < 0.05$ ). Bivariate relationship between SOC and other soil  
281 physical, chemical properties and vegetation characteristics are presented in the supplementary Fig.  
282 A.2.

### 283 **3.4. Relationship of SOC with soil and vegetation properties**

284 SOC content was positively correlated with tree DBH, tree height, organic C: N, latitude, and longitude,  
285 but negatively correlated with soil salinity, bulk density, soil pH, tree density and elevation ( $p < 0.05$ )  
286 (Fig. 7). As total nitrogen and species richness did not show any significant correlation with SOC  
287 content, these two parameters were discarded from the subsequent PCA analysis. The measured  
288 properties also showed a significant positive and negative correlation among themselves, which  
289 indicates a source of multicollinearity, a phenomenon which makes multiple regression unreliable.  
290 Therefore, principal component analysis was used to identify and group those properties that influence  
291 SOC the most and to overcome the influence of multicollinearity.

292 Principal component analysis (PCA) was performed with ten variables to assemble and isolate the  
293 smallest possible of subsets to explain the variation of the dataset (Fig. 8). The PCA result indicates that  
294 the first two principal components explained more than two-thirds of the total variation with an  
295 eigenvalue greater than 1. The most important component (PC1) explained 49.5% with the highest

296 loadings (>0.35) for soil SS (soil salinity) and pH. On the other hand, the second component showed  
297 higher loadings for tree H, DBH and soil C: N with 20% explained variation (Table A.7). As soil SS  
298 and pH are highly correlated with each other ( $r = 0.76, p < 0.05$ ) (Fig. 7), the variable with the highest  
299 loading, soil SS, was selected from the first component for the regression model. Similarly, tree H was  
300 discarded due to collinearity with tree DBH and therefore, tree DBH and soil C: N was selected from  
301 the second component.

302 By using the PCA-derived subset of variables, the relationship between SOC and soil and vegetation  
303 properties was obtained by using stepwise multiple linear regression (MLR). The regression results  
304 showed that soil salinity alone could explain 50% SOC variability in the Sundarbans, however, the  
305 percentage increases to 57% and 62% when soil C: N or soil C: N and tree DBH are added to the model  
306 (Table 3). Although all three regression models are highly significant (Table A.8), the best subset of  
307 MLR model was selected based on the largest adjusted  $R^2$  value and the smallest Mallow's Cp, AIC  
308 (Akaike Information Criteria) and RMSE (Root Mean Squared Error) and presented in Eq.1.

309 
$$\text{Ln (SOC)} = 3.439 - 0.077 \text{ SS} + 0.274 \text{ Ln (C: N)} + 0.017 \text{ DBH} \dots \dots \dots \text{Eq. 1}$$

#### 4. Discussion

310 The reported average soil organic carbon (SOC) density in this study is lower than previous estimates  
311 from the Sundarbans and far lower than average estimates of SOC density from global mangroves  
312 (Table 1). SOC density, the standardized carbon stock measurement with depth, is the most useful  
313 parameter to compare SOC between different forests (Donato et al., 2011; Weiss et al., 2016). However,  
314 due to unreported bulk density, it was not possible to convert from the reported organic carbon (%) to  
315 SOC density for most of the local and world studies. Despite a greater range of soil organic carbon  
316 (SOC) percentage in this study (0.3 – 4.4%), the average value (1.2 %) is in line with most previous  
317 studies, although higher than estimates published by Ray et al. (2011), Banerjee et al. (2012), and  
318 Allison et al. (2003). These differences are likely to be attributed to variable sampling strategies along  
319 with variable soil depth or different methods used for carbon estimation. Likewise SOC density, the  
320 average top 1m SOC storage in the Bangladesh Sundarbans ( $50.9 \pm 15.2 \text{ Mg ha}^{-1}$ ) is almost half of the  
321 previous estimate by Rahman et al. (2015), Sanderman et al. (2018) and Atwood et al. (2017). Estimates

322 of soil organic carbon could fluctuate based on the differences in sampling design, choice of analytical  
323 method and soil depth (Howard et al., 2014; Nayak et al., 2019). In the case of mangroves, Passos et al.  
324 (2016) found overestimation of organic carbon measured with the oxidation method in comparison to  
325 the elemental analyser. Anaerobic microbial decomposition yields reduced soil compounds (i.e.,  $\text{Fe}^{2+}$ ,  
326  $\text{S}^{2-}$ ,  $\text{Mn}^{2+}$ , and  $\text{Cl}^-$ ) in mangroves, which might interfere with organic carbon determination with  
327 chemical oxidation method (Nelson and Sommers, 1996; Bisutti et al., 2004; De Vos et al., 2007;  
328 Nóbrega et al., 2015). Apart from using different methods, the SOC variation originates from the  
329 consideration of soil depth in sample design as the SOC concentration is a function of soil depth and  
330 shows considerable variability (Wuest, 2009; Kauffman and Donato, 2012; Jandl et al., 2014).  
331 Moreover, using coring for sampling might have an influence on soil bulk density estimation leading to  
332 lower SOC stock estimation in deeper soils (Rau et al., 2011; Gross and Harrison, 2018).

333 In comparison to global studies, the estimated top 1m SOC stock is lower in the Sundarbans than the  
334 reported average from sites distributed all over the world (Table 1). Based on model-based  
335 georeferenced database of mangrove SOC, the global SOC map showed that the Sundarbans contains  
336 the lowest SOC stocks per ha in the world (Sanderman et al., 2018). Compared to direct estimates from  
337 190 sites across the world by Kauffman et al. (2020), the Sundarbans contains higher SOC than only  
338 two other mangrove forests, the Porto Céu mangrove in Brazil ( $48 \text{ Mg ha}^{-1}$ ) and the Bu Tinah Janoub  
339 in the United Arab Emirates ( $33 \text{ Mg ha}^{-1}$ ), located in lower and higher latitudes respectively than the  
340 Sundarbans. However, global comparison in soil carbon among tropical, subtropical and temperate  
341 mangroves showed a contrasting relationship with latitudes (Atwood et al., 2017; Twilley et al., 2018;  
342 Kauffman et al., 2020; Ouyang and Lee, 2020). Both Kauffman et al. (2020) and Ouyang and Lee  
343 (2020) found significantly lower soil carbon in mangroves  $>20^\circ\text{N}$ , although the former study had fewer  
344 samples largely limited to the middle east hyper arid mangroves. On the other hand, Atwood et al.  
345 (2017) and Twilley et al. (2018) documented the poor relationship between latitude and SOC stocks.  
346 This poor relationship might be attributed due to the poor representation of samples in the studies from  
347 the subtropical mangroves like the Sundarbans.

348 The low soil carbon in the Sundarbans is largely due to high mineral sediment deposition (Sanderman  
349 et al., 2018; Twilley et al., 2018), low burial rate (Ray et al., 2011), rapid turnover rate (Ray et al.,  
350 2018), historical logging, stand age (Marchand, 2017), plant litter quality (Rovai et al., 2018) and  
351 biological processes. Being both a tide and river-dominated ecosystem, the carbon allocation in the  
352 above and below ground is very complex, largely dependent on the local and regional geomorphic and  
353 geophysical drivers (Twilley et al., 2018). In riverine deltas, trees invest much of the carbon to the  
354 above ground to keep pace with sedimentation and sea-level rise, which is evident in the oligohaline  
355 zone with greater forest productivity (Twilley et al., 2018; Sarker et al., 2019a; Sarker et al., 2019b).  
356 Moreover, research has highlighted that mangroves subjected to frequent cyclones leading to temporary  
357 losses of above ground carbon are usually followed by rapid below ground carbon gains during recovery  
358 process according to the ‘Ecosystem Development’ theory (Odum, 1969; Danielson et al., 2017;  
359 Kominoski et al., 2018). These rapid carbon gains in the above ground and the disturbance from the  
360 catastrophic cyclones could be the source of higher autochthonous input to the below ground.  
361 Nonetheless, higher tidal amplitude in the Sundarbans leads to higher carbon export totalling 7.3 Tg C  
362  $\text{yr}^{-1}$  to the adjacent Bay of Bengal, which is higher than any other mangroves in the world (Ray et al.,  
363 2018). This rapid carbon turnover results in reduced burial of organic matter (0.18%) in the soil (Ray  
364 et al., 2011). Moreover, the pronounced tidal cycles in the Sundarbans affects carbon burial process by  
365 altering soil water chemistry (Chatterjee et al., 2013; Spivak et al., 2019). Besides high carbon turnover  
366 rate, the Sundarbans is believed to have become tidally active in the recent past due to reduced  
367 freshwater flow from the Ganges-Brahmaputra-Meghna river (Rogers et al., 2013; Hale et al., 2019).  
368 However, despite the historical reduction of sedimentation, the Sundarbans is itself still keeping pace  
369 with sea-level rise with the highest average surface elevation and vertical accretion rate (0.74 and 2.71  
370  $\text{cm yr}^{-1}$ ) compared to the worldwide average (Bomer et al., 2020a; Bomer et al., 2020b). This high  
371 sedimentation rate is the outcome of the massive flux of clastic sediments which attenuates the amount  
372 of organic carbon per unit area.

373 The century-long historical exploitation in the Sundarbans before the felling moratorium in 1989 has  
374 largely decreased the populations of threatened tree species (Siddiqi, 2001; Sarker et al., 2011). This in

375 turn is likely to have lessened the continuous autochthonous input of organic matter in the forest and  
376 reduced the overall stand age. Studies also showed that historical harvesting had altered the species  
377 composition in the Sundarbans, with decreasing abundances of *Heritiera fomes*, *Ceriops decandra* and  
378 *Xylocarpus mekongensis* and increasing for *Excoecaria agallocha* (Sarker et al., 2016). The SOC stock  
379 also depends on the age of the stands as evident in the Chrono sequence study on SOC stocks in French  
380 Guiana which revealed that the SOC varied from 4 to 107 Mg ha<sup>-1</sup> from young stand to senescent stage  
381 (Marchand, 2017). In addition, studies have suggested that lower organic carbon in the soil is mostly  
382 associated with higher C: N of the plant litter which has resulted from lowering decomposition speed  
383 and decreasing carbon-use efficiency of the decomposer (Bouillon et al., 2003; Zhou et al., 2019).  
384 Compared to mangrove associates, the senescent leaves of true mangroves contain considerably higher  
385 C: N (~33) in the Indian part of Sundarbans (Chanda et al., 2016a). Kamruzzaman et al. (2019) observed  
386 a decreasing trend of C: N of the leaf litter in both forest floor and buried condition starting from 40,  
387 but barely reached below 30 after 196 days of decomposition study, suggesting N limitation in the  
388 oligohaline zone of the Bangladesh Sundarbans. The low organic carbon can also be attributed by the  
389 abundance of leaf-consuming organisms ingesting organic litter detritus both at surface and subsurface  
390 in burrows. The Sundarbans encompasses a wide range of gastropod species (e.g., *Cerithedia cingulata*,  
391 *Cymia lacera*) that predominantly consume mangrove detritus (Nayak et al., 2014).

392 Variation in SOC stocks among different forest types is often mediated by the primary productivity,  
393 resources allocation in different parts (e.g. above and below ground) and microorganism activity is  
394 driven by a number of biological (e.g. bioturbation and species composition) and physical (e.g. soil  
395 texture, salinity, inundation and nutrients) factors (McLeod et al., 2011). Therefore, differing stand  
396 structure and composition of mangrove forests in different tidal regimes yield variable SOC stock  
397 (Lacerda et al., 1995; Gleason and Ewel, 2002). Moreover, the long and short-term resilience and  
398 resistance of microbial communities are largely dependent on the structure and zonation of mangrove  
399 communities reflecting environmental gradients (Capdeville et al., 2019). In this study, the species with  
400 higher SOC stock such as *Bruguiera* sp., *Sonneratia* sp. and *Avicennia* sp. are frequently inundated due  
401 to proximity to the river and low land than other species in the Sundarbans (Siddiqi, 2001; Sarker et al.,

2016). These high inundation regimes, in turn, lead to increased microbial activity and a higher level of dissolved organic carbon in the sediment (Wang et al., 2013; Chambers et al., 2014; Chambers et al., 2016). Regular tides also bring sediments along with high allochthonous input whereas the raised less-inundated areas foster autochthonous SOC and less microbial activity (Lovell et al., 2015; Woodroffe et al., 2016). Rao et al. (1994) found almost double C: N ratio in fresh leaves of *Bruguiera* sp. compared with other mangrove species, suggesting higher input of autochthonous carbon. Being the pioneer species in the succession of the Sundarbans, both *Sonneratia* sp. and *Avicennia* sp. are resilient to disturbances leading to higher SOC than climax and seral species (Table A.1) and accumulate a large quantity of organic litter in the tidal channel close to the river or seafront (Sarker et al., 2016; Bomer et al., 2020a). The variability of SOC stocks among forest types followed a similar pattern to the global studies by Atwood et al. (2017), except for *Sonneratia* sp. which was found to hold less SOC stock than *Heritiera* and *Ceriops*. On the other hand, Kauffman et al. (2020) found significantly lower below ground carbon stocks in *Avicennia* sp., especially in the arid mangroves of Middle-East Asia, which is solely occupied by this species. Therefore, the impact of above ground vegetation of below ground is largely site-specific, and it depends on a wide range of factors.

The unexplained variation of the best multiple regression models ( $R^2 = 0.64$ ) highlights the necessity of including other soil and environmental parameters such as soil cations and anions, clay characteristics and texture, precipitation, temperature, and river discharge. This study did not address these properties and suggests future studies incorporate a wider range of parameters to gain a better understating of organic carbon dynamics in the Sundarbans. In particular, for better ecosystem management, future research should include information relating to contextualising soil (e.g. soil texture, grain size and minerology), biogeochemical (e.g. important properties of soil and pore-water chemistry such as sulphate, oxygen, nitrate, ferric oxides in case of mangroves) and ecological (e.g. vegetation and plant-microbe interaction) properties (Luo et al., 2019; Spivak et al., 2019). However, soil salinity is considered as the outcome of the combined impact of these climatic and environmental variables in the Sundarbans resulting pronounced differences of SOC stock among the three salinity zones (Sarker et al., 2016; Sarker et al., 2019b; Rahman et al., 2020). Several previous studies have confirmed that

429 salinity determines the strong zonation of tree species and diversity in the Sundarbans, which in turn  
430 leads to comparatively higher diversity and taller tree species in the oligohaline followed by mesohaline  
431 and polyhaline zone (Aziz and Paul, 2015; Sarker et al., 2016; Sarker et al., 2019a; Sarker et al., 2019b;  
432 Rahman et al., 2020). Comparatively higher productive trees (e.g. higher DBH and higher height)  
433 promotes organic matter accumulation through producing higher litter mass and increases SOC stock  
434 by forming stable aggregates from roots and pneumatophores (Lange et al., 2015). The three salinity  
435 zones also comprise differential soil physical, chemical properties and vegetation characteristics that  
436 usually affects SOC storage by influencing microbial decomposition, soil water chemistry, plant-  
437 microbe interaction, and plant litter quality. While comparing nutrient concentration in the leaf litter of  
438 *Sonneratia apetala*, one of the major pioneer species in the Sundarbans, Nasrin et al. (2019) found  
439 lowest concentrations of N, P and K and the highest concentrations of Na in the polyhaline zone,  
440 reflecting higher C: N in the leaf litter. However, the low SOC in the polyhaline zone is also coincided  
441 with the low C: N indicting inwelling of marine and terrestrial suspended particulate materials (Bouillon  
442 et al., 2003). The strong positive correlation ( $r = 0.66$ ,  $p < 0.001$ ) between carbon and nitrogen density  
443 indicates that the source of carbon and nitrogen is likely to be same and can vary spatially (Matsui et  
444 al., 2015).

445 Although the Sundarbans is considered to be of recent origin, the large accommodation space exists due  
446 to accretion and erosion with historical relative sea-level variability (Goodbred and Kuehl, 2000; Tyagi  
447 and Sen, 2019). Therefore, the Sundarbans might have a 3m organic layer in the seaward direction and  
448 much more in the landward (Allison et al., 2003). By considering this vertical depth and the area covered  
449 by mangrove forest, the Sundarbans are likely to contain considerable volumes of soil organic carbon.  
450 Previous research has demonstrated that mangroves holding higher carbon storage also have a higher  
451 rate of deforestation with 50 % mangrove loss attributed to Indonesia, which holds about 25% of soil  
452 carbon in the world's mangroves; the figure increases to 75% when Malaysia and Myanmar are  
453 considered (Atwood et al., 2017). Therefore, mangroves from these countries are considered as a  
454 significant source of emissions due to high deforestation and forest conversion (Hamilton and Friess,  
455 2018). On the other hand, in Bangladesh, despite the lower SOC stock in the Sundarbans mangrove

456 forest demonstrated by this paper, recent positive trends in forest cover demonstrate the value of blue  
457 carbon conservation and an improved understanding of carbon storage will be of benefit to the inclusion  
458 of mangroves in national and international climate strategies and policies.

## 5. Conclusion

459 The top meter of soil organic carbon (SOC) per area in the Bangladesh Sundarbans is lower than has  
460 previously been reported. However, the total SOC will likely to be greater if total vertical depth is  
461 considered. The soil organic carbon stock (SOC) in the Sundarbans is largely influenced by soil salinity,  
462 probably by amending the forest productivity and microbial activity. The results highlighted that  
463 increasing salinity as result of predicted sea-level rise will likely have pronounced effects on future soil  
464 carbon accumulation rates by altering the soil environment and vegetation characteristics. The study  
465 underlines the importance of spatial conservation planning measures and initiatives to conserve and  
466 maximize carbon accumulation and to contribute to global climate change adaptation and mitigation  
467 strategies. Results suggest that high sediment carbon zone in the eastern part of the Sundarbans is highly  
468 vulnerable to tourism and economic development activities. In terms of climate change mitigation and  
469 adaptation, the conservation of the existing carbon stock should receive much higher priority rather than  
470 the debates of high-low carbon stock. The Bangladesh Sundarbans can act as an important blue carbon  
471 hotspot due to the high sedimentation and carbon sequestration rate and conservation priority by the  
472 government. However, disturbances such as sea-level rise, global warming, eutrophication, and  
473 landscape development might hinder this conservation activities in the future.

474

## 475 Funding

476 The study was funded by Commonwealth Scholarship Commission in the UK (Grant number: BDCS-  
477 2017-55).

## 478 Conflict of interest

479 The authors agreed that they have no conflict of interest.

480 **Acknowledgements**

481 We are grateful to Commonwealth Scholarship Commission in the UK for the PhD scholarship to the  
482 first author. We want to extend our gratitude to the Bangladesh Forest Department for giving permission  
483 for fieldwork in the Sundarbans and Forestry and Wood Technology Discipline, Khulna University for  
484 allowing study leave to the first author. We also thank everyone involved the fieldwork in the  
485 Sundarbans and we recognised that without their help, this work could not have been completed. We  
486 are also grateful to the Institute of Hazard, Risk and Resilience for a small research grant and the  
487 Department of Geography, Durham University for allowing laboratory analysis and to Ustinov College,  
488 Durham University for a travel grant. Lastly, we give thanks to Ms. Robyn Shilland for her brilliant  
489 comments in the manuscript.

## References

- 490 Abdullah, A.N., Stacey, N., Garnett, S.T., Myers, B., 2016. Economic dependence on mangrove forest  
491 resources for livelihoods in the Sundarbans, Bangladesh. *For. Policy Econ.* 64, 15-24.  
492 <https://doi.org/10.1016/j.forpol.2015.12.009>.
- 493 Alam, M., 1989. Geology and depositional history of Cenozoic sediments of the Bengal Basin of  
494 Bangladesh. *Palaeogeogr., Palaeoclimatol., Palaeoecol.* 69, 125-139.  
495 [https://doi.org/10.1016/0031-0182\(89\)90159-4](https://doi.org/10.1016/0031-0182(89)90159-4).
- 496 Allison, M., Kepple, E., 2001. Modern sediment supply to the lower delta plain of the Ganges-  
497 Brahmaputra River in Bangladesh. *Geo-Mar. Lett.* 21, 66-74.  
498 <https://doi.org/10.1007/s003670100069>.
- 499 Allison, M.A., Khan, S.R., Goodbred, S.L., Kuehl, S.A., 2003. Stratigraphic evolution of the late  
500 Holocene Ganges–Brahmaputra lower delta plain. *Sediment. Geol.* 155, 317-342.  
501 [https://doi.org/10.1016/S0037-0738\(02\)00185-9](https://doi.org/10.1016/S0037-0738(02)00185-9).
- 502 Alongi, D.M., 2012. Carbon sequestration in mangrove forests. *Carbon Management.* 3, 313-322.  
503 <https://doi.org/10.4155/cmt.12.20>.
- 504 Alongi, D.M., 2014. Carbon Cycling and Storage in Mangrove Forests. *Ann. Rev. Mar. Sci.* 6, 195-  
505 219. <https://doi.org/10.1146/annurev-marine-010213-135020>.
- 506 Atwood, T.B., Connolly, R.M., Almahasheer, H., Carnell, P.E., Duarte, C.M., Lewis, C.J.E., Irigoien,  
507 X., Kelleway, J.J., Lavery, P.S., Macreadie, P.I., Serrano, O., Sanders, C.J., Santos, I., Steven,  
508 A.D.L., Lovelock, C.E., 2017. Global patterns in mangrove soil carbon stocks and losses. *Nat.*  
509 *Climate Change.* 7, 523-528. <https://doi.org/10.1038/nclimate3326>.
- 510 Aziz, A., Paul, A.R., 2015. Bangladesh Sundarbans: Present status of the Environment and Biota.  
511 *Diversity.* 7, 242-269. <https://doi.org/10.3390/d7030242>.
- 512 Baldwin, D.S., Rees, G.N., Mitchell, A.M., Watson, G., Williams, J., 2006. The short-term effects of  
513 salinization on anaerobic nutrient cycling and microbial community structure in sediment from  
514 a freshwater wetland. *Wetlands.* 26, 455-464. [https://doi.org/10.1672/0277-5212\(2006\)26\[455:TSEOSO\]2.0.CO;2](https://doi.org/10.1672/0277-5212(2006)26[455:TSEOSO]2.0.CO;2).
- 516 Banerjee, K., Bal, G., Mitra, A., 2018. How soil texture affects the organic carbon load in the mangrove  
517 ecosystem? A case study from Bhitarkanika, Odisha. in: Singh, V.P., Yadav, S., Yadava, R.N.  
518 (Eds.), *Environmental Pollution*. Springer Singapore, Singapore, pp. 329-341.
- 519 Banerjee, K., Roy Chowdhury, M., Sengupta, K., Sett, S., Mitra, A., 2012. Influence of anthropogenic  
520 and natural factors on the mangrove soil of Indian Sundarbans wetland. *Archives of*  
521 *Environmental Science.* 6, 80-91.
- 522 Bisutti, I., Hilke, I., Raessler, M., 2004. Determination of total organic carbon – an overview of current  
523 methods. *TrAC Trends in Analytical Chemistry.* 23, 716-726.  
524 <https://doi.org/10.1016/j.trac.2004.09.003>.
- 525 Bomer, E.J., Wilson, C.A., Elsey-Quirk, T., 2020a. Process Controls of the Live Root Zone and Carbon  
526 Sequestration Capacity of the Sundarbans Mangrove Forest, Bangladesh. *Sci.* 2, 35.  
527 <https://doi.org/10.3390/sci2020035>.
- 528 Bomer, E.J., Wilson, C.A., Hale, R.P., Hossain, A.N.M., Rahman, F.M.A., 2020b. Surface elevation  
529 and sedimentation dynamics in the Ganges-Brahmaputra tidal delta plain, Bangladesh:  
530 Evidence for mangrove adaptation to human-induced tidal amplification. *Catena.* 187, 104312.  
531 <https://doi.org/10.1016/j.catena.2019.104312>.
- 532 Bouillon, S., Boschker, H.T.S., 2006. Bacterial carbon sources in coastal sediments: a cross-system  
533 analysis based on stable isotope data of biomarkers. *Biogeosciences.* 3, 175-185.  
534 <https://doi.org/10.5194/bg-3-175-2006>.
- 535 Bouillon, S., Dahdouh-Guebas, F., Rao, A.V.V.S., Koedam, N., Dehairs, F., 2003. Sources of organic  
536 carbon in mangrove sediments: variability and possible ecological implications. *Hydrobiologia.*  
537 495, 33-39. <https://doi.org/10.1023/a:1025411506526>.
- 538 Brodersen, K.E., Trevathan-Tackett, S.M., Nielsen, D.A., Connolly, R.M., Lovelock, C.E., Atwood,  
539 T.B., Macreadie, P.I., 2019. Oxygen consumption and sulfate reduction in vegetated coastal  
540 habitats: effects of physical disturbance. *Front. Mar. Sci.* 6, 00014.  
541 <https://doi.org/10.3389/fmars.2019.00014>.

542 Capdeville, C., Pommier, T., Gervais, J., Fromard, F., Rols, J.-L., Leflaive, J., 2019. Mangrove Facies  
543 Drives Resistance and Resilience of Sediment Microbes Exposed to Anthropogenic Disturbance.  
544 *Frontiers in Microbiology*. 9. <https://doi.org/10.3389/fmicb.2018.03337>.

545 Chaffey, D.R., Miller, F.R., Sandom, J.H., 1985. A forest inventory of the Sundarbans, Bangladesh.  
546 Project Report No.140, Overseas Development Authority (ODA), London.

547 Chambers, L.G., Davis, S.E., Troxler, T., Boyer, J.N., Downey-Wall, A., Scinto, L.J., 2014.  
548 Biogeochemical effects of simulated sea level rise on carbon loss in an Everglades mangrove  
549 peat soil. *Hydrobiologia*. 726, 195-211. <https://doi.org/10.1007/s10750-013-1764-6>.

550 Chambers, L.G., Guevara, R., Boyer, J.N., Troxler, T.G., Davis, S.E., 2016. Effects of Salinity and  
551 Inundation on Microbial Community Structure and Function in a Mangrove Peat Soil.  
552 *Wetlands*. 36, 361-371. <https://doi.org/10.1007/s13157-016-0745-8>.

553 Chanda, A., Akhand, A., Manna, S., Das, S., Mukhopadhyay, A., Das, I., Hazra, S., Choudhury, S.B.,  
554 Rao, K.H., Dadhwal, V.K., 2016a. Mangrove associates versus true mangroves: a comparative  
555 analysis of leaf litter decomposition in Sundarban. *Wetlands Ecol. Manage.* 24, 293-315.  
556 <https://doi.org/10.1007/s11273-015-9456-9>.

557 Chanda, A., Mukhopadhyay, A., Ghosh, T., Akhand, A., Mondal, P., Ghosh, S., Mukherjee, S., Wolf,  
558 J., Lázár, A.N., Rahman, M.M., Salehin, M., Chowdhury, S.M., Hazra, S., 2016b. Blue carbon  
559 stock of the Bangladesh Sundarban mangroves: What could be the scenario after a century?  
560 *Wetlands*. 36, 1033-1045. <https://doi.org/10.1007/s13157-016-0819-7>.

561 Chatterjee, M., Shankar, D., Sen, G., Sanyal, P., Sundar, D., Michael, G., Chatterjee, A., Amol, P.,  
562 Mukherjee, D., Suprit, K., 2013. Tidal variations in the Sundarbans estuarine system, India. *J.*  
563 *Earth Syst. Sci.* 122, 899-933.

564 Chowdhury, M.Q., De Ridder, M., Beeckman, H., 2016. Climatic signals in tree rings of *Heritiera*  
565 *fomes* Buch.-Ham. in the Sundarbans, Bangladesh. *Plos One*. 11, e0149788.  
566 <https://doi.org/10.1371/journal.pone.0149788>.

567 Craft, C., 2007. Freshwater input structures soil properties, vertical accretion, and nutrient accumulation  
568 of Georgia and U.S. tidal marshes. *Limnol. Oceanogr.* 52, 1220-1230.  
569 <https://doi.org/10.4319/lo.2007.52.3.1220>.

570 Danielson, T.M., Rivera-Monroy, V.H., Castañeda-Moya, E., Briceño, H., Travieso, R., Marx, B.D.,  
571 Gaiser, E., Farfán, L.M., 2017. Assessment of Everglades mangrove forest resilience:  
572 Implications for above-ground net primary productivity and carbon dynamics. *For. Ecol.*  
573 *Manage.* 404, 115-125. <https://doi.org/10.1016/j.foreco.2017.08.009>.

574 De Vos, B., Lettens, S., Muys, B., Deckers, J.A., 2007. Walkley–Black analysis of forest soil organic  
575 carbon: recovery, limitations and uncertainty. *Soil Use and Management*. 23, 221-229.  
576 <https://doi.org/10.1111/j.1475-2743.2007.00084.x>.

577 Donato, D.C., Kauffman, J.B., Murdiyarsa, D., Kurnianto, S., Stidham, M., Kanninen, M., 2011.  
578 Mangroves among the most carbon-rich forests in the tropics. *Nat. Geosci.* 4, 293-297.  
579 <https://doi.org/10.1038/ngeo1123>.

580 Duarte, C.M., Losada, I.J., Hendriks, I.E., Mazarrasa, I., Marbà, N., 2013. The role of coastal plant  
581 communities for climate change mitigation and adaptation. *Nat. Climate Change*. 3, 961-968.  
582 <https://doi.org/10.1038/nclimate1970>.

583 Dutta, J., Banerjee, K., Agarwal, S., Mitra, A., 2019. Soil Organic Carbon (SOC): A Proxy to Assess the  
584 Degree of Anthropogenic and Natural Stress. *The Journal of Interrupted Studies* 2, 90-102

585 Dutta, M.K., Chowdhury, C., Jana, T.K., Mukhopadhyay, S.K., 2013. Dynamics and exchange fluxes  
586 of methane in the estuarine mangrove environment of the Sundarbans, NE coast of India.  
587 *Atmospheric Environment* 77, 631-639. <https://doi.org/10.1016/j.atmosenv.2013.05.050>

588 Fontaine, S., Barot, S., Barré, P., Bdioui, N., Mary, B., Rumpel, C., 2007. Stability of organic carbon  
589 in deep soil layers controlled by fresh carbon supply. *Nature*. 450, 277-280.  
590 <https://doi.org/10.1038/nature06275>.

591 Fox, J., Weisberg, S., 2019. An R companion to applied regression, Third ed. Sage, Thousand Oaks  
592 CA.

593 Freeman, C., Ostle, N.J., Fenner, N., Kang, H., 2004. A regulatory role for phenol oxidase during  
594 decomposition in peatlands. *Soil Biol. Biochem.* 36, 1663-1667.  
595 <https://doi.org/10.1016/j.soilbio.2004.07.012>.

596 Friess, D.A., Rogers, K., Lovelock, C.E., Krauss, K.W., Hamilton, S.E., Lee, S.Y., Lucas, R.,  
597 Primavera, J., Rajkaran, A., Shi, S., 2019. The State of the World's Mangrove Forests: Past,  
598 Present, and Future. *Annu. Rev. Env. Resour.* 44, 89-115. [https://doi.org/10.1146/annurev-  
600 environ-101718-033302](https://doi.org/10.1146/annurev-<br/>
599 environ-101718-033302).

600 Friess, D.A., Yando, E.S., Abuchahla, G.M.O., Adams, J.B., Cannicci, S., Canty, S.W.J., Cavanaugh,  
601 K.C., Connolly, R.M., Cormier, N., Dahdouh-Guebas, F., Diele, K., Feller, I.C., Fratini, S.,  
602 Jennerjahn, T.C., Lee, S.Y., Ogurcak, D.E., Ouyang, X., Rogers, K., Rowntree, J.K., Sharma,  
603 S., Sloey, T.M., Wee, A.K.S., 2020. Mangroves give cause for conservation optimism, for now.  
604 *Curr. Biol.* 30, R153-R154. <https://doi.org/10.1016/j.cub.2019.12.054>.

605 Giri, C., Ochieng, E., Tieszen, L.L., Zhu, Z., Singh, A., Loveland, T., Masek, J., Duke, N., 2011. Status  
606 and distribution of mangrove forests of the world using earth observation satellite data. *Global  
607 Ecol. Biogeogr.* 20, 154-159. <https://doi.org/10.1111/j.1466-8238.2010.00584.x>.

608 Gleason, S.M., Ewel, K.C., 2002. Organic matter dynamics on the forest floor of a micronesia  
609 mangrove forest: An investigation of species composition shifts. *Biotropica.* 34, 190-198.  
610 <https://doi.org/10.1111/j.1744-7429.2002.tb00530.x>.

611 Goodbred, S.L., Kuehl, S.A., 2000. The significance of large sediment supply, active tectonism, and  
612 eustasy on margin sequence development: Late Quaternary stratigraphy and evolution of the  
613 Ganges–Brahmaputra delta. *Sediment. Geol.* 133, 227-248. [https://doi.org/10.1016/S0037-  
615 0738\(00\)00041-5](https://doi.org/10.1016/S0037-<br/>
614 0738(00)00041-5).

615 Gross, C.D., Harrison, R.B., 2018. Quantifying and Comparing Soil Carbon Stocks: Underestimation  
616 with the Core Sampling Method. *Soil Sci. Soc. Am. J.* 82, 949-959.  
617 <https://doi.org/10.2136/sssaj2018.01.0015>.

618 Hale, R., Bain, R., Goodbred Jr, S., Best, J., 2019. Observations and scaling of tidal mass transport  
619 across the lower Ganges–Brahmaputra delta plain: implications for delta management and  
620 sustainability. *Earth Surface Dynamics.* 7, 231-245. <https://doi.org/10.5194/esurf-7-231-2019>.

621 Hamilton, S.E., Friess, D.A., 2018. Global carbon stocks and potential emissions due to mangrove  
622 deforestation from 2000 to 2012. *Nat. Climate Change.* 8, 240-244.  
623 <https://doi.org/10.1038/s41558-018-0090-4>.

624 Hardie, M., Doyle, R., 2012. Measuring Soil Salinity. in: Shabala, S., Cuin, T.A. (Eds.), *Plant Salt  
625 Tolerance: Methods and Protocols.* Humana Press, Totowa, NJ, pp. 415-425.  
626 [https://doi.org/10.1007/978-1-61779-986-0\\_28](https://doi.org/10.1007/978-1-61779-986-0_28).

627 Hawker, L., Neal, J., Bates, P., 2019. Accuracy assessment of the TanDEM-X 90 Digital Elevation  
628 Model for selected floodplain sites. *Remote Sens. Environ.* 232, 111319.  
629 <https://doi.org/10.1016/j.rse.2019.111319>.

630 Hossain, G.M., Bhuiyan, M.A.H., 2016. Spatial and temporal variations of organic matter contents and  
631 potential sediment nutrient index in the Sundarbans mangrove forest, Bangladesh. *KSCE  
632 Journal of Civil Engineering.* 20, 163-174. <https://doi.org/10.1007/s12205-015-0333-0>.

633 Howard, J., Hoyt, S., Isensee, K., Telszewski, M., Pidgeon, E. (Eds.), 2014. Coastal blue carbon:  
634 methods for assessing carbon stocks and emissions factors in mangroves, tidal salt marshes,  
635 and seagrasses. Conservation International, Intergovernmental Oceanographic Commission of  
636 UNESCO, International Union for Conservation of Nature, Arlington, Virginia, USA, pp. 184.

637 Hu, Y., Wang, L., Fu, X., Yan, J., Wu, J., Tsang, Y., Le, Y., Sun, Y., 2016. Salinity and nutrient contents  
638 of tidal water affects soil respiration and carbon sequestration of high and low tidal flats of  
639 Jiuduansha wetlands in different ways. *Sci. Total Environ.* 565, 637-648.  
640 <https://doi.org/10.1016/j.scitotenv.2016.05.004>.

641 Iftekhar, M., Saenger, P., 2008. Vegetation dynamics in the Bangladesh Sundarbans mangroves: a  
642 review of forest inventories. *Wetlands Ecol. Manage.* 16, 291-312.  
643 <https://doi.org/10.1007/s11273-007-9063-5>.

644 IPCC, 2014. 2013 Supplement to the 2006 IPCC guidelines for national greenhouse gas inventories:  
645 Wetlands. in: Hiraishi, T. et al. (Eds.). IPCC, Geneva, Switzerland, pp. 354.

646 Islam, M.R., Begum, S.F., Yamaguchi, Y., Ogawa, K., 1999. The Ganges and Brahmaputra rivers in  
647 Bangladesh: basin denudation and sedimentation. *Hydrological Processes.* 13, 2907-2923.  
648 [https://doi.org/10.1002/\(sici\)1099-1085\(19991215\)13:17<2907::Aid-hyp906>3.0.Co;2-e](https://doi.org/10.1002/(sici)1099-1085(19991215)13:17<2907::Aid-hyp906>3.0.Co;2-e).

649

- 650 Islam, S.N., 2016. Deltaic floodplains development and wetland ecosystems management in the  
651 Ganges–Brahmaputra–Meghna Rivers Delta in Bangladesh. *Sustainable Water Resources*  
652 *Management*. 2, 237-256. <https://doi.org/10.1007/s40899-016-0047-6>.
- 653 Jackson, D.A., 1993. Stopping Rules in Principal Components Analysis: A Comparison of Heuristical  
654 and Statistical Approaches. *Ecology*. 74, 2204-2214. <https://doi.org/10.2307/1939574>.
- 655 Jandl, R., Rodeghiero, M., Martinez, C., Cotrufo, M.F., Bampa, F., van Wesemael, B., Harrison, R.B.,  
656 Guerrini, I.A., Richter, D.d., Rustad, L., Lorenz, K., Chabbi, A., Miglietta, F., 2014. Current  
657 status, uncertainty and future needs in soil organic carbon monitoring. *Sci. Total Environ*. 468-  
658 469, 376-383. <https://doi.org/10.1016/j.scitotenv.2013.08.026>.
- 659 Jardine, S.L., Siikamäki, J.V., 2014. A global predictive model of carbon in mangrove soils.  
660 *Environmental Research Letters*. 9, 104013. <https://doi.org/10.1088/1748-9326/9/10/104013>.
- 661 Kamruzzaman, M., Basak, K., Paul, S.K., Ahmed, S., Osawa, A., 2019. Litterfall production,  
662 decomposition and nutrient accumulation in Sundarbans mangrove forests, Bangladesh. *Forest*  
663 *Science and Technology*. 15, 24-32. <https://doi.org/10.1080/21580103.2018.1557566>.
- 664 Kauffman, J.B., Adame, M.F., Arifanti, V.B., Schile-Beers, L.M., Bernardino, A.F., Bhomia, R.K.,  
665 Donato, D.C., Feller, I.C., Ferreira, T.O., Jesus Garcia, M.d.C., MacKenzie, R.A., Megonigal,  
666 J.P., Murdiyarso, D., Simpson, L., Hernández Trejo, H., 2020. Total ecosystem carbon stocks  
667 of mangroves across broad global environmental and physical gradients. *Ecol. Monogr*. 90.  
668 <https://doi.org/10.1002/ecm.1405>.
- 669 Kauffman, J.B., Donato, D., 2012. Protocols for the measurement, monitoring and reporting of  
670 structure, biomass and carbon stocks in mangrove forests. Working Paper 86. Center for  
671 International Forestry Research (CIFOR), Bogor, Indonesia, pp. 50.
- 672 Khan, M., Amin, M., 2019. Macro nutrient status of Sundarbans forest soils in southern region of  
673 Bangladesh. *Bangladesh Journal of Scientific and Industrial Research*. 54, 67-72.  
674 <https://doi.org/10.3329/bjsir.v54i1.40732>.
- 675 Kominoski, J.S., Gaiser, E.E., Baer, S.G., 2018. Advancing Theories of Ecosystem Development  
676 through Long-Term Ecological Research. *Bioscience*. 68, 554-562.  
677 <https://doi.org/10.1093/biosci/biy070>.
- 678 Krauss, K.W., McKee, K.L., Lovelock, C.E., Cahoon, D.R., Saintilan, N., Reef, R., Chen, L., 2014.  
679 How mangrove forests adjust to rising sea level. *New Phytol*. 202, 19-34.  
680 <https://doi.org/10.1111/nph.12605>.
- 681 Kristensen, E., Bouillon, S., Dittmar, T., Marchand, C., 2008. Organic carbon dynamics in mangrove  
682 ecosystems: A review. *Aquat. Bot*. 89, 201-219. <https://doi.org/10.1016/j.aquabot.2007.12.005>.
- 683 Lacerda, L.D., Ittekkot, V., Patchineelam, S.R., 1995. Biogeochemistry of mangrove soil organic  
684 matter: a comparison between *Rhizophora* and *Avicennia* soils in south-eastern Brazil. *Estuar.*  
685 *Coast. Shelf Sci*. 40, 713-720. <https://doi.org/10.1006/ecss.1995.0048>.
- 686 Lange, M., Eisenhauer, N., Sierra, C.A., Bessler, H., Engels, C., Griffiths, R.I., Mellado-Vázquez, P.G.,  
687 Malik, A.A., Roy, J., Scheu, S., Steinbeiss, S., Thomson, B.C., Trumbore, S.E., Gleixner, G.,  
688 2015. Plant diversity increases soil microbial activity and soil carbon storage. *Nature*  
689 *Communications*. 6, 6707. <https://doi.org/10.1038/ncomms7707>.
- 690 Legendre, P., Legendre, L.F., 2012. Numerical ecology, Third ed. Elsevier, Great Britain, pp. 1006.
- 691 Liu, X., Ruecker, A., Song, B., Xing, J., Conner, W.H., Chow, A.T., 2017. Effects of salinity and wet-  
692 dry treatments on C and N dynamics in coastal-forested wetland soils: Implications of sea level  
693 rise. *Soil Biol. Biochem*. 112, 56-67. <https://doi.org/10.1016/j.soilbio.2017.04.002>.
- 694 Liu, Z., Lee, C., 2006. Drying effects on sorption capacity of coastal sediment: The importance of  
695 architecture and polarity of organic matter. *Geochim. Cosmochim. Acta*. 70, 3313-3324.  
696 <https://doi.org/10.1016/j.gca.2006.04.017>.
- 697 Lovelock, C.E., Cahoon, D.R., Friess, D.A., Guntenspergen, G.R., Krauss, K.W., Reef, R., Rogers, K.,  
698 Saunders, M.L., Sidik, F., Swales, A., Saintilan, N., Thuyen, L.X., Triet, T., 2015. The  
699 vulnerability of Indo-Pacific mangrove forests to sea-level rise. *Nature*. 526, 559-563.  
700 <https://doi.org/10.1038/nature15538>.
- 701 Lovelock, C.E., Duarte, C.M., 2019. Dimensions of Blue Carbon and emerging perspectives. *Biol. Lett*.  
702 15, 20180781. <https://doi.org/10.1098/rsbl.2018.0781>.

703 Lovelock, C.E., Sorrell, B.K., Hancock, N., Hua, Q., Swales, A., 2010. Mangrove Forest and Soil  
704 Development on a Rapidly Accreting Shore in New Zealand. *Ecosystems*. 13, 437-451.  
705 <https://doi.org/10.1007/s10021-010-9329-2>.

706 Luo, M., Huang, J.-F., Zhu, W.-F., Tong, C., 2019. Impacts of increasing salinity and inundation on  
707 rates and pathways of organic carbon mineralization in tidal wetlands: a review. *Hydrobiologia*.  
708 827, 31-49. <https://doi.org/10.1007/s10750-017-3416-8>.

709 Macreadie, P.I., Anton, A., Raven, J.A., Beaumont, N., Connolly, R.M., Friess, D.A., Kelleway, J.J.,  
710 Kennedy, H., Kuwae, T., Lavery, P.S., Lovelock, C.E., Smale, D.A., Apostolaki, E.T., Atwood,  
711 T.B., Baldock, J., Bianchi, T.S., Chmura, G.L., Eyre, B.D., Fourqurean, J.W., Hall-Spencer,  
712 J.M., Huxham, M., Hendriks, I.E., Krause-Jensen, D., Laffoley, D., Luisetti, T., Marbà, N.,  
713 Masque, P., McGlathery, K.J., Magonigal, J.P., Murdiyarso, D., Russell, B.D., Santos, R.,  
714 Serrano, O., Silliman, B.R., Watanabe, K., Duarte, C.M., 2019. The future of Blue Carbon  
715 science. *Nature Communications*. 10, 3998. <https://doi.org/10.1038/s41467-019-11693-w>.

716 Marchand, C., 2017. Soil carbon stocks and burial rates along a mangrove forest chronosequence  
717 (French Guiana). *For. Ecol. Manage.* 384, 92-99. <https://doi.org/10.1016/j.foreco.2016.10.030>.

718 Marton, J.M., Herbert, E.R., Craft, C.B., 2012. Effects of Salinity on Denitrification and Greenhouse  
719 Gas Production from Laboratory-incubated Tidal Forest Soils. *Wetlands*. 32, 347-357.  
720 <https://doi.org/10.1007/s13157-012-0270-3>.

721 Matsui, N., Meepol, W., Chukwamdee, J., 2015. Soil Organic Carbon in Mangrove Ecosystems with  
722 Different Vegetation and Sedimentological Conditions. *Journal of Marine Science and*  
723 *Engineering*. 3, 1404-1424. <https://doi.org/10.3390/jmse3041404>.

724 McLeod, E., Chmura, G.L., Bouillon, S., Salm, R., Björk, M., Duarte, C.M., Lovelock, C.E.,  
725 Schlesinger, W.H., Silliman, B.R., 2011. A blueprint for blue carbon: toward an improved  
726 understanding of the role of vegetated coastal habitats in sequestering CO<sub>2</sub>. *Front. Ecol.*  
727 *Environ.* 9, 552-560. <https://doi.org/10.1890/110004>.

728 Mitra, A., Banerjee, K., Sett, S., 2012. Spatial Variation in Organic Carbon Density of Mangrove Soil  
729 in Indian Sundarbans. *National Academy Science Letters* 35, 147-154.  
730 <https://doi.org/10.1007/s40009-012-0046-6>.

731 Morrissey, E.M., Gillespie, J.L., Morina, J.C., Franklin, R.B., 2014. Salinity affects microbial activity  
732 and soil organic matter content in tidal wetlands. *Global Change Biol.* 20, 1351-1362.  
733 <https://doi.org/10.1111/gcb.12431>.

734 Nasrin, S., Hossain, M., Rahman, M.M., 2019. Adaptive responses to salinity: nutrient resorption  
735 efficiency of *Sonneratia apetala* (Buch.-Ham.) along the salinity gradient in the Sundarbans of  
736 Bangladesh. *Wetlands Ecol. Manage.* 27, 343-351. [https://doi.org/10.1007/s11273-019-09663-](https://doi.org/10.1007/s11273-019-09663-6)  
737 [6](https://doi.org/10.1007/s11273-019-09663-6).

738 Nayak, A.K., Rahman, M.M., Naidu, R., Dhal, B., Swain, C.K., Nayak, A.D., Tripathi, R., Shahid, M.,  
739 Islam, M.R., Pathak, H., 2019. Current and emerging methodologies for estimating carbon  
740 sequestration in agricultural soils: A review. *Sci. Total Environ.* 665, 890-912.  
741 <https://doi.org/10.1016/j.scitotenv.2019.02.125>.

742 Nayak, B., Zaman, S., Gadi, S.D., Raha, A.K., Mitra, A., 2014. Dominant gastropods of Indian  
743 Sundarbans: A major sink of carbon. *International Journal of Advances in Pharmacy, Biology*  
744 *and Chemistry*. 3, 282-289.

745 Nellemann, C., Corcoran, E., Duarte, C., Valdés, L., De Young, C., Fonseca, L., Grimsditch, G. (Eds.),  
746 2009. Blue carbon. A rapid response assessment. United Nations Environment Programme  
747 (UNEP), GRID-Arendal, pp. 78.

748 Nelson, D.W., Sommers, L.E., 1996. Total carbon, organic carbon, and organic matter. in: Sparks, D.  
749 et al. (Eds.), *Methods of soil analysis: Part 3 Chemical methods*, pp. 961-1010.  
750 <https://doi.org/10.2136/sssabookser5.3.c34>.

751 Nóbrega, G.N., Ferreira, T.O., Artur, A.G., de Mendonça, E.S., de O. Leão, R.A., Teixeira, A.S., Otero,  
752 X.L., 2015. Evaluation of methods for quantifying organic carbon in mangrove soils from semi-  
753 arid region. *J. Soils Sed.* 15, 282-291. <https://doi.org/10.1007/s11368-014-1019-9>.

754 Nyman, J.A., Delaune, R.D., Patrick, W.H., 1990. Wetland soil formation in the rapidly subsiding  
755 Mississippi River Deltaic Plain: Mineral and organic matter relationships. *Estuar. Coast. Shelf*  
756 *Sci.* 31, 57-69. [https://doi.org/10.1016/0272-7714\(90\)90028-P](https://doi.org/10.1016/0272-7714(90)90028-P).

- 757 Odum, E.P., 1969. The strategy of ecosystem development. *Science*. 164, 262-270.  
758 <https://doi.org/10.1126/science.164.3877.262>.
- 759 Ouyang, X., Lee, S.Y., 2020. Improved estimates on global carbon stock and carbon pools in tidal  
760 wetlands. *Nature Communications*. 11, 317. <https://doi.org/10.1038/s41467-019-14120-2>.
- 761 Passos, T.R.G., Artur, A.G., Nóbrega, G.N., Otero, X.L., Ferreira, T.O., 2016. Comparison of the  
762 quantitative determination of soil organic carbon in coastal wetlands containing reduced forms  
763 of Fe and S. *Geo-Mar. Lett.* 36, 223-233. <https://doi.org/10.1007/s00367-016-0437-7>.
- 764 Pendleton, L., Donato, D.C., Murray, B.C., Crooks, S., Jenkins, W.A., Sifleet, S., Craft, C., Fourqurean,  
765 J.W., Kauffman, J.B., Marbà, N., Megonigal, P., Pidgeon, E., Herr, D., Gordon, D., Baldera,  
766 A., 2012. Estimating Global “Blue Carbon” Emissions from Conversion and Degradation of  
767 Vegetated Coastal Ecosystems. *PLOS ONE*. 7, e43542.  
768 <https://doi.org/10.1371/journal.pone.0043542>.
- 769 Prasad, M.B.K., Kumar, A., Ramanathan, A.L., Datta, D.K., 2017. Sources and dynamics of  
770 sedimentary organic matter in Sundarban mangrove estuary from Indo-Gangetic delta.  
771 *Ecological Processes* 6, 8. <https://doi.org/10.1186/s13717-017-0076-6>.
- 772 R Core Team, 2019. R: A language and environment for statistical computing. R Foundation for  
773 Statistical Computing, Vienna, Austria.
- 774 Rahman, M.M., Khan, M.N.I., Hoque, A.K.F., Ahmed, I., 2015. Carbon stock in the Sundarbans  
775 mangrove forest: spatial variations in vegetation types and salinity zones. *Wetlands Ecol.*  
776 *Manage.* 23, 269-283. <https://doi.org/10.1007/s11273-014-9379-x>.
- 777 Rahman, M.S., Sass-Klaassen, U., Zuidema, P.A., Chowdhury, M.Q., Beeckman, H., 2020. Salinity  
778 drives growth dynamics of the mangrove tree *Sonneratia apetala* Buch. -Ham. in the  
779 Sundarbans, Bangladesh. *Dendrochronologia*. 62, 125711.  
780 <https://doi.org/10.1016/j.dendro.2020.125711>.
- 781 Rao, R.G., Woitchik, A.F., Goeyens, L., van Riet, A., Kazungu, J., Dehairs, F., 1994. Carbon, nitrogen  
782 contents and stable carbon isotope abundance in mangrove leaves from an east African coastal  
783 lagoon (Kenya). *Aquat. Bot.* 47, 175-183. [https://doi.org/10.1016/0304-3770\(94\)90012-4](https://doi.org/10.1016/0304-3770(94)90012-4).
- 784 Rath, K.M., Rousk, J., 2015. Salt effects on the soil microbial decomposer community and their role in  
785 organic carbon cycling: A review. *Soil Biol. Biochem.* 81, 108-123.  
786 <https://doi.org/10.1016/j.soilbio.2014.11.001>.
- 787 Rau, B.M., Melvin, A.M., Johnson, D.W., Goodale, C.L., Blank, R.R., Fredriksen, G., Miller, W.W.,  
788 Murphy, J.D., Todd, D.E.J., Walker, R.F., 2011. Revisiting Soil Carbon and Nitrogen  
789 Sampling: Quantitative Pits Versus Rotary Cores. *Soil Science*. 176, 273-279.  
790 <https://doi.org/10.1097/SS.0b013e31821d6d4a>.
- 791 Ray, R., Baum, A., Rixen, T., Gleixner, G., Jana, T.K., 2018. Exportation of dissolved (inorganic and  
792 organic) and particulate carbon from mangroves and its implication to the carbon budget in the  
793 Indian Sundarbans. *Sci. Total Environ.* 621, 535-547.  
794 <https://doi.org/10.1016/j.scitotenv.2017.11.225>.
- 795 Ray, R., Ganguly, D., Chowdhury, C., Dey, M., Das, S., Dutta, M.K., Mandal, S.K., Majumder, N., De,  
796 T.K., Mukhopadhyay, S.K., Jana, T.K., 2011. Carbon sequestration and annual increase of  
797 carbon stock in a mangrove forest. *Atmos. Environ.* 45, 5016-5024.  
798 <https://doi.org/10.1016/j.atmosenv.2011.04.074>.
- 799 Ren, H., Jian, S., Lu, H., Zhang, Q., Shen, W., Han, W., Yin, Z., Guo, Q., 2008. Restoration of mangrove  
800 plantations and colonisation by native species in Leizhou bay, South China. *Ecol. Res.* 23, 401-  
801 407. <https://doi.org/10.1007/s11284-007-0393-9>.
- 802 Rogers, K., Kelleway, J.J., Saintilan, N., Megonigal, J.P., Adams, J.B., Holmquist, J.R., Lu, M., Schile-  
803 Beers, L., Zawadzki, A., Mazumder, D., Woodroffe, C.D., 2019. Wetland carbon storage  
804 controlled by millennial-scale variation in relative sea-level rise. *Nature*. 567, 91-95.  
805 <https://doi.org/10.1038/s41586-019-0951-7>.
- 806 Rogers, K.G., Goodbred, S.L., Mondal, D.R., 2013. Monsoon sedimentation on the ‘abandoned’ tide-  
807 influenced Ganges–Brahmaputra delta plain. *Estuar. Coast. Shelf Sci.* 131, 297-309.  
808 <https://doi.org/10.1016/j.ecss.2013.07.014>.
- 809 Rovai, A.S., Twilley, R.R., Castañeda-Moya, E., Riul, P., Cifuentes-Jara, M., Manrow-Villalobos, M.,  
810 Horta, P.A., Simonassi, J.C., Fonseca, A.L., Pagliosa, P.R., 2018. Global controls on carbon

811 storage in mangrove soils. *Nat. Climate Change*. 8, 534-538. [https://doi.org/10.1038/s41558-](https://doi.org/10.1038/s41558-018-0162-5)  
812 018-0162-5.

813 Rudra, K., 2014. Changing river courses in the western part of the Ganga–Brahmaputra delta.  
814 *Geomorphology*. 227, 87-100. <https://doi.org/10.1016/j.geomorph.2014.05.013>.

815 Sanderman, J., Hengl, T., Fiske, G., Solvik, K., Adame, M.F., Benson, L., Bukoski, J.J., Carnell, P.,  
816 Cifuentes-Jara, M., Donato, D., Duncan, C., Eid, E.M., Ermgassen, P.z., Lewis, C.J.E.,  
817 Macreadie, P.I., Glass, L., Gress, S., Jardine, S.L., Jones, T.G., Nsombo, E.N., Rahman, M.M.,  
818 Sanders, C.J., Spalding, M., Landis, E., 2018. A global map of mangrove forest soil carbon at  
819 30 m spatial resolution. *Environmental Research Letters*. 13. [https://doi.org/10.1088/1748-](https://doi.org/10.1088/1748-9326/aabe1c)  
820 9326/aabe1c.

821 Sarker, S.K., Deb, J.C., Halim, M.A., 2011. A diagnosis of existing logging bans in Bangladesh.  
822 *International Forestry Review*. 13, 461-475. <https://doi.org/10.1505/146554811798811344>.

823 Sarker, S.K., Matthiopoulos, J., Mitchell, S.N., Ahmed, Z.U., Mamun, M.B.A., Reeve, R., 2019a.  
824 1980s–2010s: The world's largest mangrove ecosystem is becoming homogeneous. *Biol.*  
825 *Conserv.* 236, 79-91. <https://doi.org/10.1016/j.biocon.2019.05.011>.

826 Sarker, S.K., Reeve, R., Paul, N.K., Matthiopoulos, J., 2019b. Modelling spatial biodiversity in the  
827 world's largest mangrove ecosystem—The Bangladesh Sundarbans: A baseline for  
828 conservation. *Divers. Distrib.* 25, 729-742. <https://doi.org/10.1111/ddi.12887>.

829 Sarker, S.K., Reeve, R., Thompson, J., Paul, N.K., Matthiopoulos, J., 2016. Are we failing to protect  
830 threatened mangroves in the Sundarbans world heritage ecosystem? *Scientific Reports*. 6.  
831 <https://doi.org/10.1038/srep21234>.

832 Setia, R., Gottschalk, P., Smith, P., Marschner, P., Baldock, J., Setia, D., Smith, J., 2013. Soil salinity  
833 decreases global soil organic carbon stocks. *Sci. Total Environ.* 465, 267-272.  
834 <https://doi.org/10.1016/j.scitotenv.2012.08.028>.

835 Siddiqi, N.A., 2001. Mangrove forestry in Bangladesh. Institute of Forestry & Environmental Sciences,  
836 University of Chittagong, Chittagong, Bangladesh, pp. 301.

837 Spivak, A.C., Sanderman, J., Bowen, J.L., Canuel, E.A., Hopkinson, C.S., 2019. Global-change controls  
838 on soil-carbon accumulation and loss in coastal vegetated ecosystems. *Nat. Geosci.* 12, 685-  
839 692. <https://doi.org/10.1038/s41561-019-0435-2>.

840 Syvitski, J.P.M., Milliman, J.D., 2007. Geology, Geography, and Humans Battle for Dominance over  
841 the Delivery of Fluvial Sediment to the Coastal Ocean. *The Journal of Geology*. 115, 1-19.  
842 <https://doi.org/10.1086/509246>.

843 Taillardat, P., Friess, D.A., Lupascu, M., 2018. Mangrove blue carbon strategies for climate change  
844 mitigation are most effective at the national scale. *Biol. Lett.* 14, 20180251.  
845 <https://doi.org/10.1098/rsbl.2018.0251>.

846 Twilley, R.R., Castañeda-Moya, E., Rivera-Monroy, V.H., Rovai, A., 2017. Productivity and Carbon  
847 Dynamics in Mangrove Wetlands. in: Rivera-Monroy, V.H., Lee, S.Y., Kristensen, E., Twilley,  
848 R.R. (Eds.), *Mangrove Ecosystems: A Global Biogeographic Perspective: Structure, Function,*  
849 *and Services*. Springer International Publishing, Cham, pp. 113-162.  
850 [https://doi.org/10.1007/978-3-319-62206-4\\_5](https://doi.org/10.1007/978-3-319-62206-4_5).

851 Twilley, R.R., Rovai, A.S., Riul, P., 2018. Coastal morphology explains global blue carbon  
852 distributions. *Front. Ecol. Environ.* 16, 503-508. <https://doi.org/10.1002/fee.1937>.

853 Tyagi, N.K., Sen, H.S., 2019. Development of Sundarbans through Estuary Management for  
854 Augmenting Freshwater Supply, Improved Drainage and Reduced Bank Erosion. in: Sen, H.S.  
855 (Ed.), *The Sundarbans: A Disaster-Prone Eco-Region: Increasing Livelihood Security*.  
856 Springer International Publishing, Cham, pp. 375-402. [https://doi.org/10.1007/978-3-030-](https://doi.org/10.1007/978-3-030-00680-8_13)  
857 00680-8\_13.

858 Wang, G., Guan, D., Peart, M.R., Chen, Y., Peng, Y., 2013. Ecosystem carbon stocks of mangrove  
859 forest in Yingluo Bay, Guangdong Province of South China. *For. Ecol. Manage.* 310, 539-546.  
860 <https://doi.org/10.1016/j.foreco.2013.08.045>.

861 Weiss, C., Weiss, J., Boy, J., Iskandar, I., Mikutta, R., Guggenberger, G., 2016. Soil organic carbon  
862 stocks in estuarine and marine mangrove ecosystems are driven by nutrient colimitation of P  
863 and N. *Ecol. Evol.* 6, 5043-56. <https://doi.org/10.1002/ece3.2258>.

864 Wickham, H., 2016. *ggplot2: Elegant Graphics for Data Analysis*. Springer-Verlag, New York.

865 Więski, K., Guo, H., Craft, C.B., Pennings, S.C., 2010. Ecosystem Functions of Tidal Fresh, Brackish,  
866 and Salt Marshes on the Georgia Coast. *Estuaries and Coasts*. 33, 161-169.  
867 <https://doi.org/10.1007/s12237-009-9230-4>.

868 Wong, V.N.L., Dalal, R.C., Greene, R.S.B., 2009. Carbon dynamics of sodic and saline soils following  
869 gypsum and organic material additions: A laboratory incubation. *Applied Soil Ecology*. 41, 29-  
870 40. <https://doi.org/10.1016/j.apsoil.2008.08.006>.

871 Wong, V.N.L., Greene, R.S.B., Dalal, R.C., Murphy, B.W., 2010. Soil carbon dynamics in saline and  
872 sodic soils: a review. *Soil Use and Management*. 26, 2-11. [https://doi.org/10.1111/j.1475-  
873 2743.2009.00251.x](https://doi.org/10.1111/j.1475-2743.2009.00251.x).

874 Woodroffe, C.D., Rogers, K., McKee, K.L., Lovelock, C.E., Mendelsohn, I.A., Saintilan, N., 2016.  
875 Mangrove Sedimentation and Response to Relative Sea-Level Rise. *Ann. Rev. Mar. Sci.* 8, 243-  
876 266. <https://doi.org/10.1146/annurev-marine-122414-034025>.

877 Wuest, S.B., 2009. Correction of Bulk Density and Sampling Method Biases Using Soil Mass per Unit  
878 Area. *Soil Sci. Soc. Am. J.* 73, 312-316. <https://doi.org/10.2136/sssaj2008.0063>.

879 Yando, E.S., Osland, M.J., Willis, J.M., Day, R.H., Krauss, K.W., Hester, M.W., 2016. Salt marsh-  
880 mangrove ecotones: using structural gradients to investigate the effects of woody plant  
881 encroachment on plant–soil interactions and ecosystem carbon pools. *J. Ecol.* 104, 1020-1031.  
882 <https://doi.org/10.1111/1365-2745.12571>.

883 Yang, J., Gao, J., Liu, B., Zhang, W., 2014. Sediment deposits and organic carbon sequestration along  
884 mangrove coasts of the Leizhou Peninsula, southern China. *Estuar. Coast. Shelf Sci.* 136, 3-10.  
885 <https://doi.org/10.1016/j.ecss.2013.11.020>.

886 Zhao, Q., Bai, J., Lu, Q., Zhang, G., 2017. Effects of salinity on dynamics of soil carbon in degraded  
887 coastal wetlands: Implications on wetland restoration. *Physics and Chemistry of the Earth, Parts  
888 A/B/C*. 97, 12-18. <https://doi.org/10.1016/j.pce.2016.08.008>.

889 Zhou, G., Xu, S., Ciais, P., Manzoni, S., Fang, J., Yu, G., Tang, X., Zhou, P., Wang, W., Yan, J., Wang,  
890 G., Ma, K., Li, S., Du, S., Han, S., Ma, Y., Zhang, D., Liu, J., Liu, S., Chu, G., Zhang, Q., Li,  
891 Y., Huang, W., Ren, H., Lu, X., Chen, X., 2019. Climate and litter C/N ratio constrain soil  
892 organic carbon accumulation. *National Science Review*. 6, 746-757.  
893 <https://doi.org/10.1093/nsr/nwz045>.

894

**Fig. 1.** Sundarbans mangrove forest, Bangladesh. Legend colour represents three major salinity zones (Chanda et al., 2016b). ESRI Basemap Sources: Esri, HERE, Garmin, FAO, NOAA, USGS, © OpenStreetMap contributors, and the GIS User Community.

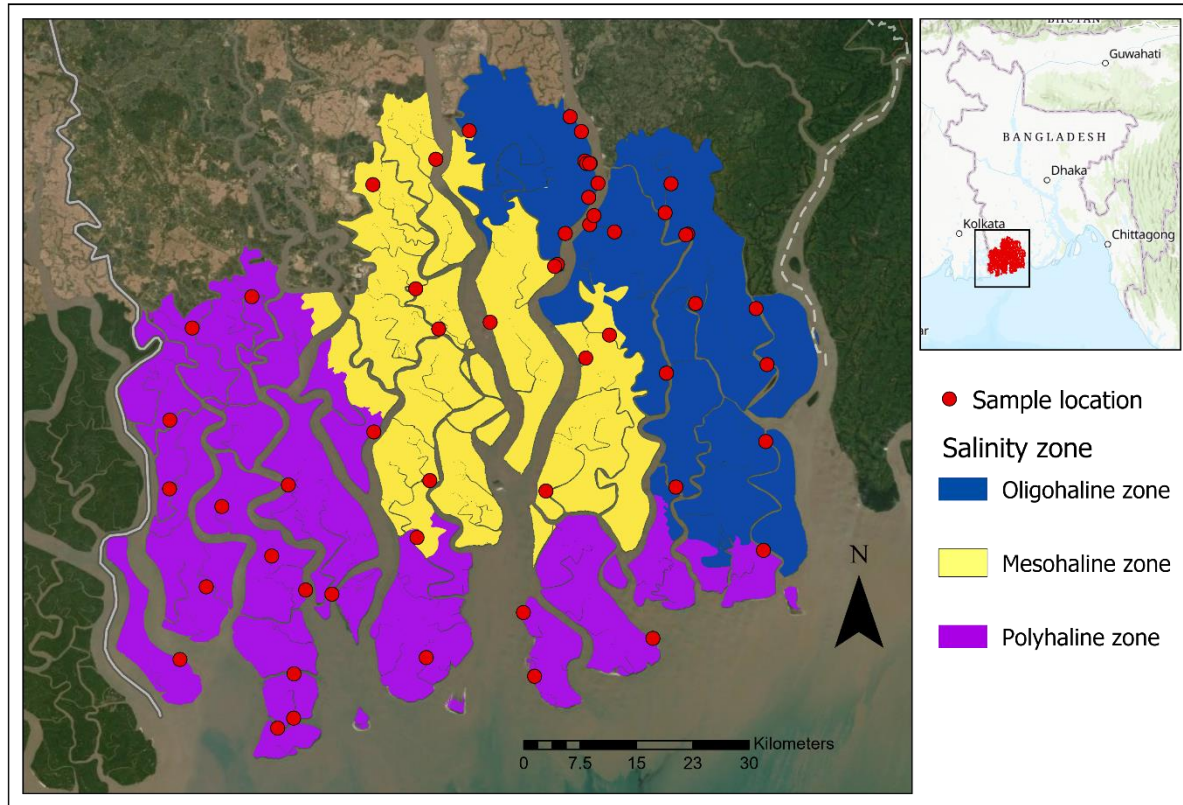


**Fig. 2.** (A) The distribution of soil organic carbon (SOC) density ( $\text{gm cm}^{-3}$ ) in four soil depths presented as violin-box plot, where the black vertical line represents the median and black dots are outliers. Here, the width of violin plot represents the proportion of the data located there as a measure of kernel probability density. (B) Average SOC density ( $\text{gm cm}^{-3}$ ) in three salinity zones and four soil depths.

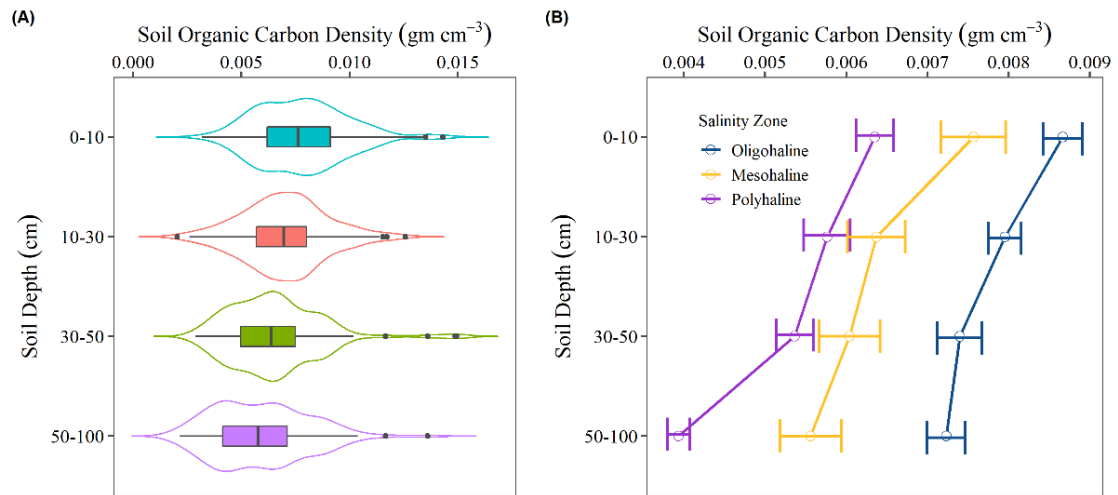


**Fig. 3.** Spatial distribution of total soil organic carbon (SOC) ( $\text{Mg ha}^{-1}$ ) and soil salinity ( $\text{dS/cm}$ ) in the Sundarbans. Note that circle represents the amount of SOC and gradual colour ramp reveals soil salinity indicating green to red as from low to high salinity. Three major salinity zones are represented according to Chanda et al., (2016b).

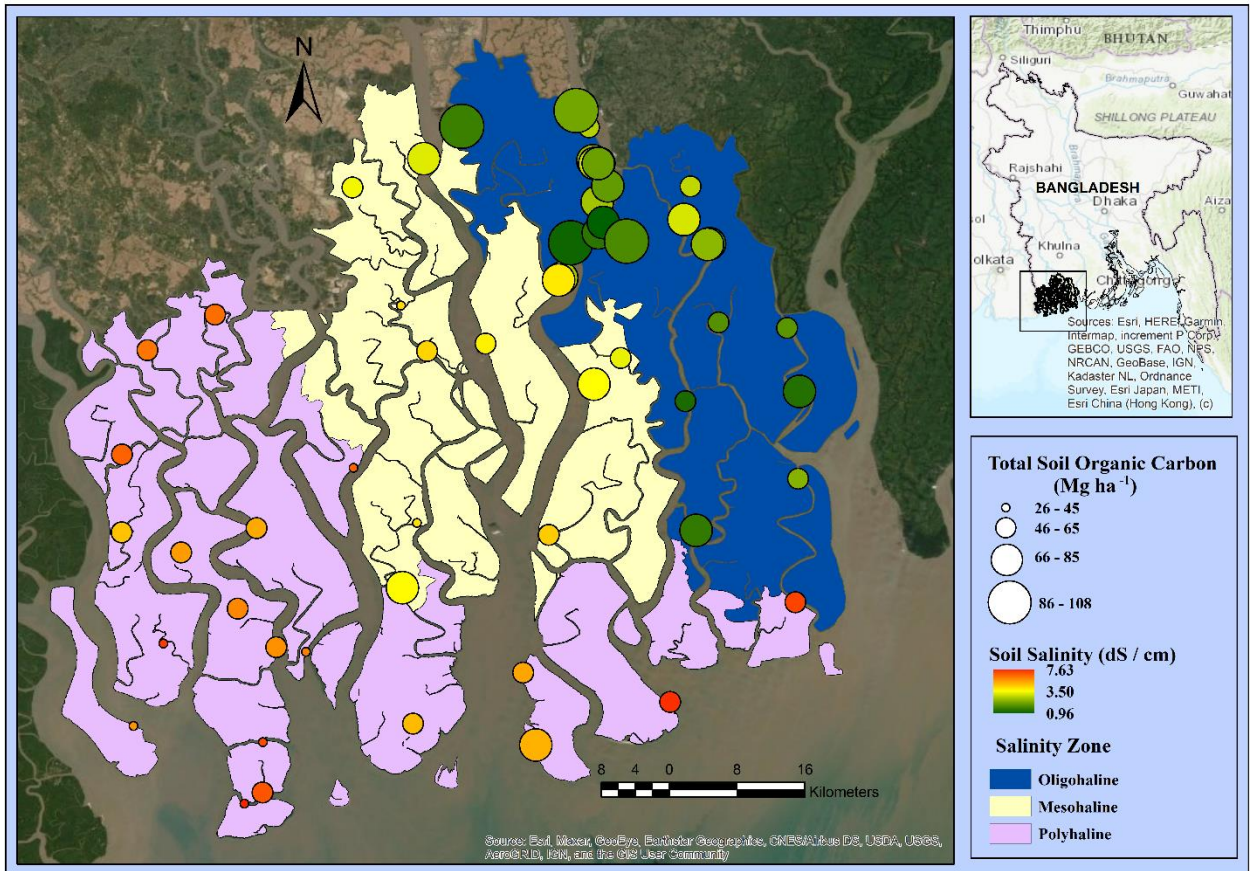


**Fig. 4.** Average soil organic carbon ( $\text{Mg ha}^{-1}$ ) in different soil depths in three salinity zones.

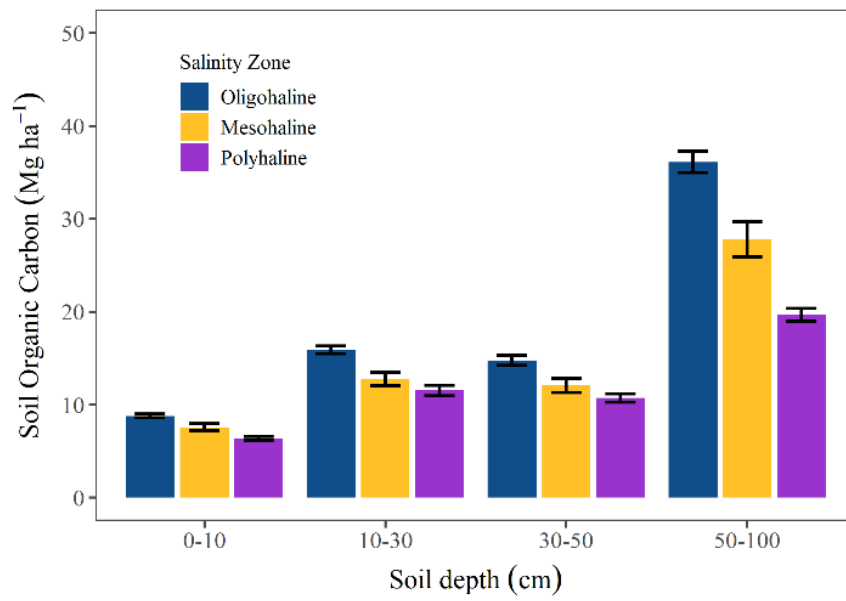


**Fig. 5.** Integrated violin-box plot shows average soil organic carbon (SOC) in major forest types in the Sundarbans. The black vertical line of box plot represents the median and the width of violin plot represents the proportion of the data located there as a measure of kernel probability density.

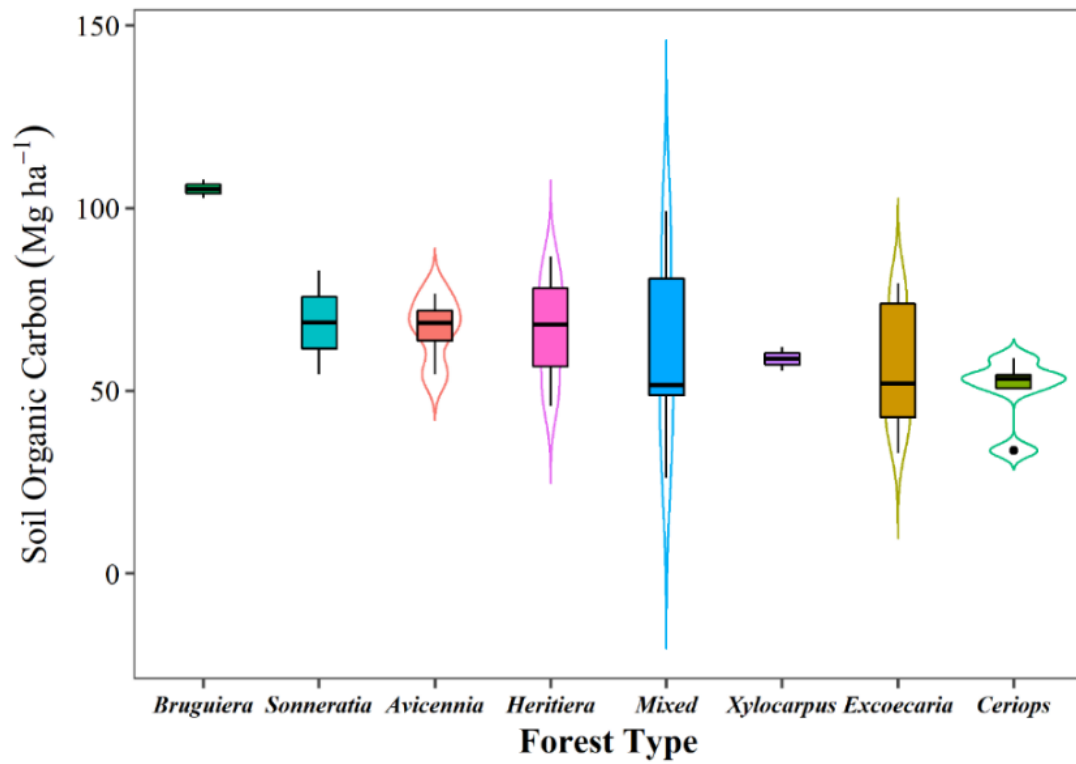


**Fig. 6.** (A) Relationship between bulk density and soil organic carbon density. (B) Relationship between soil nitrogen density and soil organic carbon density.

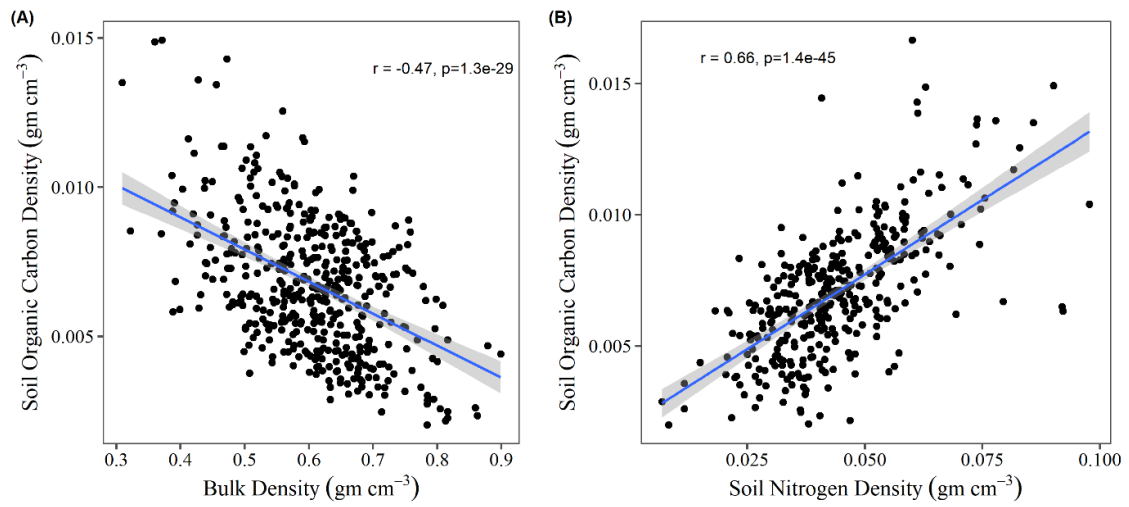




**Fig. 8.** Principal component analysis (PCA) biplot of soil physicochemical, geophysical and vegetation characteristics as vectors (n = 10) and mangroves areas are coloured coded as three salinity zones (n = 55). The soil physicochemical properties included SS= soil salinity, pH= soil pH, BD = Bulk density, C: N = organic C- total Nitrogen ratio, geophysical properties comprised LAT = Latitude, LONG= Longitude, E= Elevation, and the vegetation characteristics included TD = Tree density, DBH = mean Diameter at Breast Height, H= Mean height. Here, perpendicular direction signifies uncorrelated relationship, while negative and positive correlated vectors are presented in the opposite vectors and small angle vectors, respectively.

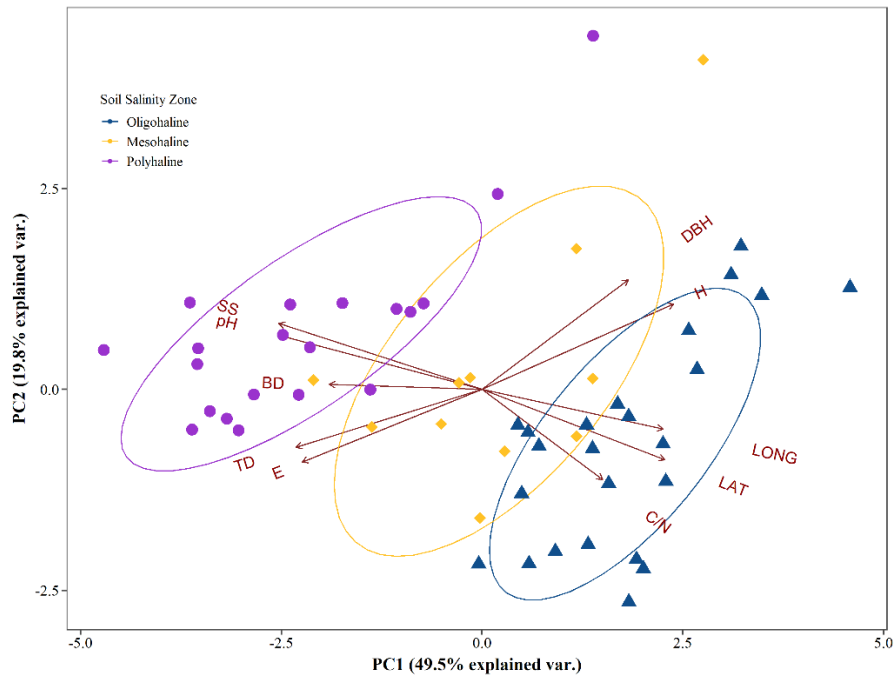


**Table 1.** Comparison of Soil Organic Carbon (SOC) density and stock among studies in the Sundarbans and globally.

Study area	Study	Sample size	Depth (cm)	Methods	Mean Soil organic carbon percentage (%) (range)	Mean Soil organic carbon density (gm/cm <sup>3</sup> ) (range)	Mean top m Soil Organic Carbon Storage (Mg/ha) (range)	
Sundarbans	Bangladesh	Bomer et al. (2020a)	56	100 cm	Coring, CHN analyser	0.9 (0.6-1.5)	0.010 (0.008-0.011)	-
		Khan and Amin (2019)	35	15 cm (0-15)	Coring, wet oxidation	0.6 (0.4 – 1.0)	-	-
		Sanderman et al. (2018)	-	100 cm	Literature and Model based	-	-	127 (74- 463)
		Atwood et al. (2017)	-	100 cm	Literature and Model based	-	-	118
		Prasad et al. (2017)	400	100 cm (1 cm interval)	Coring, CN analyser	1.25 (0.8 – 2.4)	-	-
		Hossain and Bhuiyan (2016)	96	5 cm (0-5)	Coring, wet oxidation	1.2 (0.6 – 2.0)	-	-
		Rahman et al. (2015)	150	100 cm (0-30, 30-100)	Coring, wet oxidation	-	0.011 (0.007 – 0.014)	112 (90 - 134)
		Donato et al., (2011)	4	100 cm (0-30, 30-100)	Coring, wet oxidation	1.7 (1.6-1.7)	0.016 (0.015–0.016)	-
		Allison et al. (2003)	4	600 cm (0-600)	Coring, CHN analyser	0.5 -1.1	-	-
	India	Dutta et al. (2019)	48	40 cm (0-10, 10-20, 20-30, 30-40)	Coring, wet oxidation	1.25 (0.8-1.6)	-	-
		Prasad et al. (2017)	300	100 cm (1 cm interval)	Coring, CN analyser	0.8-5.2	-	-
		Dutta et al. (2013)	15	25 cm (0-5, 5-10, 10-15,15-20, 20-25)	Coring, TOC analyser	1.8 (1.2 - 2.1)	0.017 (0.013 – 0.019)	-
		Banerjee et al. (2012)	140	40 cm (0-10, 10-20, 20-30, 30-40)	Coring, wet oxidation	1.0 (0.5 – 1.4)	0.011 (0.007 – 0.015)	-
		Mitra et al. (2012)	120	40 cm (0-10, 10-20, 20-30, 30-40) cm	Coring, wet oxidation	0.7 (0.4 – 1.1)	0.009 (0.006 – 0.012)	-
		Ray et al. (2011)	16	30 cm (0-30)	Coring, wet oxidation	0.6 (0.5-0.7)	-	-
Global studies	Kauffman et al. (2020)	190 sample plot data from 5 continents in different soil depth			-	-	334 (33 – 789)	
	Sanderman et al. (2018)	Model based estimation of carbon from literature values of 1812 samples			-	-	361 (94-628)	
	Rovai et al. (2018)	Model based estimation of carbon from literature values of 932 samples			-	0.033 (0.001 – 0.153)	-	
	Atwood et al. (2017)	Literature based estimation from 1230 sampling locations			-	-	283 (15 – 1527)	
	IPCC (2014)	Literature based estimation			-	-	428	
	Jardine and Siikamäki (2014)	Model based estimation of carbon from literature values of 932 samples			5.7 (0.1 – 43.3)	0.032 (0.014 – 0.115)	369 (272 – 703)	
	Donato et al. (2011)	Field based data from Indo-pacific area of 25 samples			11.9 (1.7 -21.5)	0.043 (0.016 – 0.076)	-	

**Table 2.** Overview of measured soil parameters and vegetation characteristics. Values are presented as mean ( $\pm$  SD), where  $n \geq 3$ . Lowercase letters indicate significant variability among salinity zones, according to least-significant difference (LSD) test at  $\alpha = 0.05$ .

Salinity zone	Bulk density (gm cm <sup>-3</sup> )	Soil pH	Soil salinity (EC dS/cm)	Total Soil Organic Carbon (Mg ha <sup>-1</sup> )	Total Nitrogen (Mg ha <sup>-1</sup> )	Organic C: N	Elevation (m)	Stem Density (ha <sup>-1</sup> )	Height (m)	DBH (Diameter at Breast Height) (cm)
<b>Oligohaline</b>	0.58 (0.07) <sup>b</sup>	7.06 (0.26) <sup>c</sup>	1.49 (0.32) <sup>c</sup>	74.77 (14.93) <sup>a</sup>	2.66 (1.19) <sup>b</sup>	21.30 (7.23) <sup>a</sup>	3.39 (1.78) <sup>b</sup>	5,009 (2,485) <sup>b</sup>	7.98 (2.03) <sup>a</sup>	8.12 (2.41) <sup>a</sup>
<b>Mesohaline</b>	0.62 (0.04) <sup>ab</sup>	7.43 (0.19) <sup>b</sup>	3.07 (0.56) <sup>b</sup>	59.30 (15.80) <sup>b</sup>	3.52 (1.08) <sup>a</sup>	17.30 (6.87) <sup>a</sup>	3.67 (1.01) <sup>ab</sup>	6,876 (3,290) <sup>ab</sup>	7.88 (2.63) <sup>a</sup>	8.60 (5.36) <sup>ab</sup>
<b>Polyhaline</b>	0.63 (0.05) <sup>a</sup>	7.80 (0.26) <sup>a</sup>	5.56 (0.85) <sup>a</sup>	48.25 (10.32) <sup>c</sup>	3.81 (0.98) <sup>a</sup>	13.08 (3.00) <sup>b</sup>	4.79 (1.52) <sup>a</sup>	8,750 (4,798) <sup>a</sup>	5.98 (1.66) <sup>b</sup>	6.72 (4.12) <sup>b</sup>

**Table 3.** Summary statistics of regression model. Here, SS = Soil salinity, C: N = Soil organic carbon: Nitrogen and DBH= tree Diameter at breast height.

<b>Model</b>	<b><math>R^2</math></b>	<b>Adjusted <math>R^2</math></b>	<b>C(p)</b>	<b>AIC</b>	<b>RMSE</b>
<b>1. SS</b>	0.508	0.498	18.217	-10.457	0.212
<b>2. SS and C: N</b>	0.590	0.574	8.650	-18.513	0.196
<b>3. SS, C: N and DBH</b>	0.637	0.616	4.00	-23.255	0.186

Table A.1. List of tree species found in the Sundarbans with taxonomy, distribution in salinity zones, inundation condition and succession stage.

Latin name	Local name	Family	Salinity zone	Inundation condition	Succession stage
<i>Aegiceras corniculatum</i> (L.) Blanco	Kholshi	Primulaceae	M, P	WL, WH	S
<i>Aglaiacucullata</i> (Roxb.) Pellegr. *	Amoor	Meliaceae	O	WH	S
<i>Avicennia alba</i> Blume.	Sada Baen	Avicenniaceae	P	WL	Pr
<i>Avicennia marina</i> (Forssk.) Vierh.	Moricha Baen	Avicenniaceae	P	WL	Pr
<i>Avicennia officinalis</i> L.	Kala Baen	Avicenniaceae	O, M, P	WL	Pr
<i>Bruguiera gymnorrhiza</i> (L.) Lam.	Lal Kakra	Rhizophoraceae	O, M, P	WL	S, C
<i>Bruguiera sexangula</i> (Lour.) Poir.	Holud Kakra	Rhizophoraceae	O, M, P	WL	S, C
<i>Cerbera manghas</i> L. *	Dakur	Apocynaceae	O	WO	S
<i>Ceriops decandra</i> (Griff.) Ding Hou	Goran	Rhizophoraceae	O, M, P	WO	C
<i>Cynometra ramiflora</i> L. *	Singra	Fabaceae	O	WH	S
<i>Excoecaria agallocha</i> L.	Gewa	Euphorbiaceae	O, M, P	WH, WO	S
<i>Excoecaria indica</i> (Willd.) Muell. Arg. *	Batul	Euphorbiaceae	O	WH	S
<i>Heritiera fomes</i> Buch. -Ham.	Sundri	Malvaceae	O, M, P	WO	C
<i>Hibiscus tiliaceus</i> L. *	Bola	Malvaceae	O, M	WH	S
<i>Intsia bijuga</i> (Colebr.) Kuntze *	Bhaila	Fabaceae	O, M	WH	S
<i>Kandelia candel</i> (L.) Druce	Vatkathi	Rhizophoraceae	M, P	WL	S
<i>Lumnitzera racemosa</i> Willd.	Kirpa	Combretaceae	P	WH, WO	S
<i>Millettia pinnata</i> (L.) Panigrahi*	Karanj	Fabaceae	O	WL	S
<i>Rhizophora apiculata</i> Blume.	Bhora Jhana	Rhizophoraceae	M, P	WL	S
<i>Rhizophora mucronata</i> Lamk.	Jhana Garjan	Rhizophoraceae	M, P	WL	S
<i>Sonneratia apetala</i> Buch. -Ham.	Keora	Lythraceae	O, M, P	WL	Pr
<i>Xylocarpus granatum</i> K.D. Koen.	Dhundul	Meliaceae	M, P	WH	S
<i>Xylocarpus mekongensis</i> Pierre.	Passur	Meliaceae	O, M, P	WH, WO	S

\* Indicates mangrove associates according to Tomlinson (2016). Abbreviation: Salinity zone- O = oligohaline, M = Mesohaline, P = Polyhaline. Inundation: WL = Waterlogged during Low tide, WH= Waterlogged during High tide, WO = Waterlogged Occasionally. Successional stage: Pr = Pioneer, S = seral and C = Climax. Source: Siddiqi (2001); Mahmood (2015); Rahman et al. (2015); Islam (2016); Sarker et al. (2016)

Table A.2 Two-way ANOVA results for SOCD (gm cm<sup>-3</sup>) in different salinity zones and soil depths.

Source	DF	SS	MSS	F	p
Soil Depth	3	6.4	2.1	30.1	<0.0001
Salinity Zone	2	15.9	7.9	112.3	<0.0001
Soil Depth*Salinity Zone	6	1.5	0.2	3.5	<0.01
Residuals	500	35.5	0.07		

Table A.3 Two-way ANOVA results for Bulk density (gm cm<sup>-3</sup>) in different salinity zones and soil depths.

Source	DF	SS	MSS	F	p
Soil Depth	3	0.9	0.3	46.2	<0.0001
Salinity Zone	2	0.3	0.2	22.2	<0.0001
Soil Depth*Salinity Zone	6	0.01	0.003	0.5	>0.5
Residuals	500	3.5	0.007		

Table A.4 Two-way ANOVA results for SOC (Mg ha<sup>-1</sup>) storage in different salinity zones and soil depths.

Source	DF	SS	MSS	F	p
Soil Depth	3	108.7	36.2	526.2	<0.0001
Salinity Zone	2	16.4	8.2	118.9	<0.0001
Soil Depth*Salinity Zone	6	1.4	0.2	3.3	<0.003
Residuals	500	34.4	0.07		

Table A.5 One-way ANOVA result for SOC in different forest types.

Source	DF	SS	MSS	F	p
Forest types	7	5704	8149	3.3	<0.01
Residuals	47	11715	249.3		

Table A.6 Tukey HSD Post-hoc test for the average soil organic carbon (SOC) (Mg ha<sup>-1</sup>) in different forest types. Different letters indicate significant differences at P<0.05. Data are mean ±Standard Deviation (SD).

Forest Types	SOC (Mg ha <sup>-1</sup> )		
	Mean	± SD	HSD rank
<i>Bruguiera sp.</i>	105.3	3.6	a
<i>Sonneratia sp.</i>	68.7	20.1	ab
<i>Avicennia sp.</i>	67.1	9.3	ab
<i>Heritiera sp.</i>	67.0	13.2	b
MIXED	61.3	28.7	b
<i>Xylocarpus sp.</i>	58.8	4.6	b
<i>Excoecaria sp.</i>	56.3	15.9	b
<i>Ceriops sp.</i>	50.2	9.7	b

Table A.7 PCA (Principal Component Analysis) results based on soil physical, chemical properties and vegetation properties. Bold values correspond highly correlated values (PCs > 0.35) and underlined values represent non-correlated variables with the respective PCs highest loading.

Principal Component	PC1	PC2
<b>Eigenvalue</b>	4.95	1.97
<b>Percentage of total variance (%)</b>	49.5	19.8
<b>Cumulative percentage (%)</b>	49.5	69.3
<b>BD</b>	-0.27	0.02
<b>pH</b>	<b>-0.36</b>	0.24
<b>SS</b>	<u><b>-0.37</b></u>	0.29
<b>TD</b>	-0.33	-0.25
<b>DBH</b>	0.26	<u><b>0.49</b></u>
<b>H</b>	0.34	<b>0.38</b>
<b>E</b>	-0.32	-0.32
<b>C/N</b>	0.21	<u><b>-0.40</b></u>
<b>LAT</b>	0.33	-0.31
<b>LONG</b>	0.32	-0.17

Table A.8 Step-wise multiple linear regression

Model		Unstandardized coefficient		Standardized coefficient	t	Significance	Lower	Upper
		$\beta$	Standard error	Beta				
<b>1</b>	(Intercept)	4.449	0.057		78.161	0.000	4.335	4.563
	Soil Salinity	-0.111	0.015	-0.712	-7.391	0.000	-0.141	-0.081
<b>2</b>	(Intercept)	3.594	0.270		13.330	0.000	3.053	4.135
	Soil Salinity	-0.083	0.016	-0.534	-5.106	0.000	-0.116	-0.050
	Ln (C: N)	0.273	0.085	0.338	3.230	0.002	0.103	0.443
<b>3</b>	(Intercept)	3.439	0.263		13.072	0.000	2.911	3.967
	Soil Salinity	-0.077	0.016	-0.499	-4.972	0.000	-0.109	-0.046
	Ln (C: N)	0.274	0.080	0.339	3.415	0.001	0.113	0.436
	Mean DBH	0.017	0.007	0.220	2.579	0.013	0.004	0.031

Dependent variable: Ln (SOC)

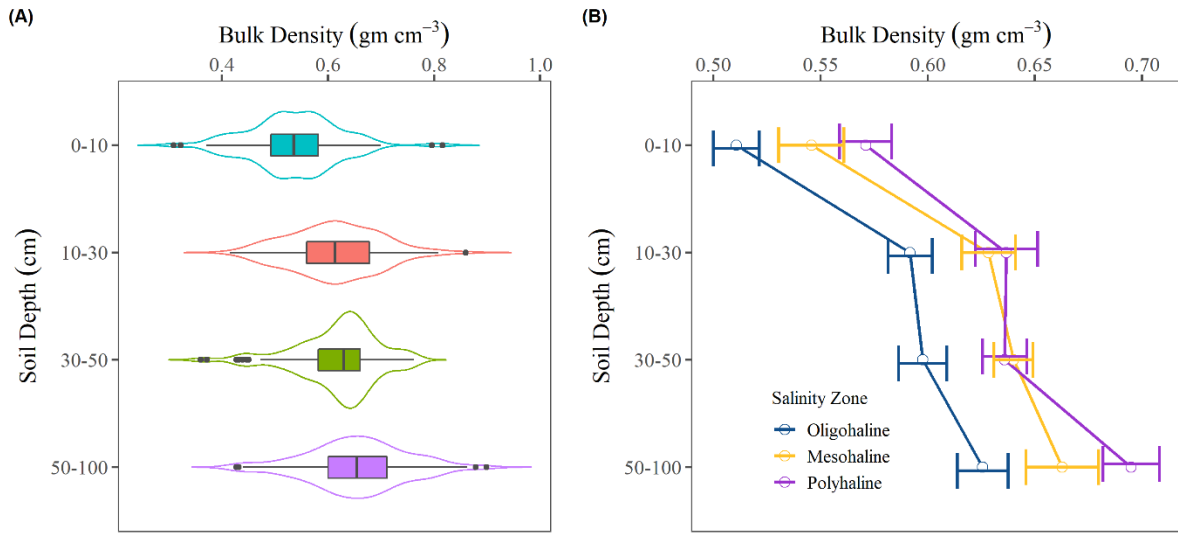


Fig. A.1. (A) Integrated violin-box plot shows the distribution of bulk density in four soil depth, where the black dots are outliers. (B) Average bulk density in three salinity zones and four soil depths.

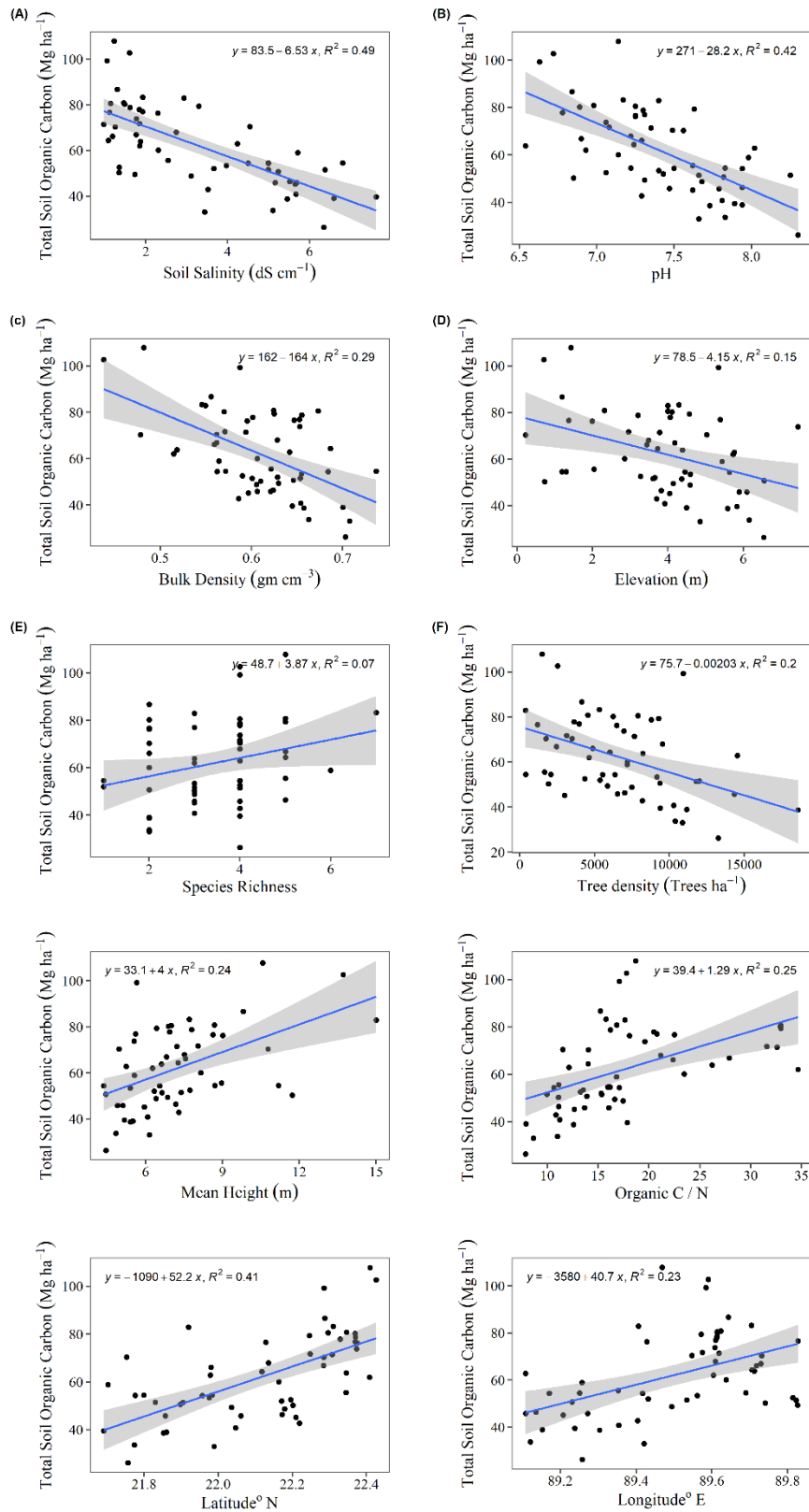


Fig. A.2. Bivariate relationship between soil organic carbon with different soil physicochemical, geophysical properties and vegetation characteristics in the Sundarbans.

### Supplementary References

- Islam, A.K.M.N., 2016. Germination eco-physiology and plant diversity in halophytes of sundarban mangrove forest in Bangladesh. in: Khan, M.A., Ozturk, M., Gul, B., Ahmed, M.Z. (Eds.), *Halophytes for Food Security in Dry Lands*. Academic Press, San Diego, pp. 277-289. <https://doi.org/10.1016/B978-0-12-801854-5.00017-0>.
- Mahmood, H., 2015. Handbook of selected plant and species of the Sundarbans and the embankment ecosystem, Sustainable Development and Biodiversity Conservation in Coastal Protection Forests, Bangladesh (SDBC-Sundarbans) Project implemented by the Deutsche Gesellschaft für Internationale Zusammenarbeit (GIZ) GmbH on behalf of the German Federal Ministry for Economic Cooperation and Development (BMZ), Dhaka.
- Rahman, M.S., Hossain, G.M., Khan, S.A., Uddin, S.N., 2015. An annotated checklist of the vascular plants of Sundarban Mangrove Forest of Bangladesh. *Bangladesh J. Plant Taxon.* 22, 17-41. <https://doi.org/10.3329/bjpt.v22i1.23862>.
- Sarker, S.K., Reeve, R., Thompson, J., Paul, N.K., Matthiopoulos, J., 2016. Are we failing to protect threatened mangroves in the Sundarbans world heritage ecosystem? *Scientific Reports.* 6. <https://doi.org/10.1038/srep21234>.
- Siddiqi, N.A., 2001. *Mangrove forestry in Bangladesh*. Institute of Forestry & Environmental Sciences, University of Chittagong, Chittagong, Bangladesh, pp. 301.
- Tomlinson, P.B., 2016. *The Botany of Mangroves*, 2 ed. Cambridge University Press, Cambridge.